

Physical Properties of Young Stellar Populations in 24 Starburst Galaxies Observed with FUSE^{*}

Anne Pellerin^{1†} and Carmelle Robert^{2‡}

¹*Space Telescope Science Institute, 3700 San Martin Drive, Baltimore, MD 21218, USA.*

²*Département de physique, de génie physique et d'optique, and Observatoire du mont Mégantic, Université Laval, Québec, QC, CANADA, G1K 7P4*

Accepted 2007 July 19. Received 2007 July 18; in original form 2007 June 15

ABSTRACT

We presents the main physical properties of very young stellar populations seen with FUSE in 24 individual starbursts. These characteristics have been obtained using the evolutionary spectral synthesis technique in the far-ultraviolet range with the `LavalSB` code. For each starburst, quantitative values for age, metallicity, initial mass function slope, stellar mass, and internal extinction have been obtained and discussed in details. Limits of the code have been tested. One main conclusion is that most starbursts (and probably all of them) cannot be represented by any continuous star formation burst in the far-ultraviolet. Also, quantitative values of various optical diagnostics related to these stellar populations have been predicted. Underlying stellar populations, dominated by B-type stars, have been detected in NGC 1140, NGC 4449, and possibly NGC 3991. We characterized the young stellar populations of less than 5 Myr in Seyfert 2 nuclei.

Key words: galaxies: evolution – galaxies: stellar content – galaxies: starburst – galaxies: Seyfert – line: profiles – ultraviolet: galaxies.

1 FUV SPECTRAL SYNTHESIS

Since the introduction of the evolutionary population synthesis technique by Tinsley (1968), many codes have been developed to work with data at various wavelength ranges, especially during the last decade (e.g. Robert, Leitherer & Heckman 1993; Worthey et al. 1994; Leitherer & Heckman 1995; Vazdekis 1999; Leitherer et al. 1999; Mollá & García-Vargas 2000; Robert et al. 2003; Bruzual & Charlot 2003). These developments are mainly due to faster computers, advances in stellar evolution theories and also to progresses in space astronomy. Spectral synthesis of young stellar populations, as observed in luminous far-infrared galaxies, nuclear starbursts, giant H II regions, and also some Seyfert nuclei (Heckman et al. 1997; González Delgado et al. 1998a; González Delgado, Heckman & Leitherer 2001), has been particularly successful in the ultraviolet from 1200 to 3000Å thanks to several space missions such as the *Hubble Space*

Telescope (HST), the *International Ultraviolet Explorer* (IUE), and the *Hopkins Ultraviolet Telescope* (HUT).

Due to important instrumental constraints for the observation of the far-ultraviolet range (FUV; $900\text{Å} < \lambda < 1200\text{Å}$), very few synthesis codes have been developed in this regime. Until recently, only the `Starburst99` code (González Delgado, Leitherer & Heckman 1997a; Leitherer et al. 1999) was including a FUV spectral library based on HUT and *Copernicus* data. The lack of spectral resolution has restricted the synthesis to O VI $\lambda\lambda 1032, 1038$, a doublet blended to Ly β and C II interstellar features. Furthermore, the low signal-to-noise ratio (S/N) of extragalactic data below 1200Å has considerably limited the application of the technique in the FUV to a very few nearby objects (e.g. Leitherer, Calzetti & Heckman 2002a).

With the launch of the *Far Ultraviolet Spectroscopic Explorer* in 1999 (FUSE; Moos et al. 2000; Sahnou et al. 2000), the FUV regime can be fully explored. Numerous O- and B-type stars have been observed and studied at those wavelengths (e.g. Crowther et al. 2002; Walborn et al. 2002; Willis et al. 2004). Comprehensive trends in the stellar line profiles of these stars have been found (Pellerin et al. 2002). Robert et al. (2003) have created new FUV spectral libraries of 228 OB stars observed with FUSE for the `LavalSB` and `Starburst99` codes. Taking advantage of the impressive spectral resolution and sensitivity of FUSE, the

^{*} Based on observations made with the NASA-CNES-CSA Far Ultraviolet Spectroscopic Explorer. FUSE is operated for NASA by the Johns Hopkins University under NASA contract NAS5-32985.

[†] E-mail: pellerin@stsci.edu

[‡] E-mail: carobert@phy.ulaval.ca

authors have shown that, in addition to the O VI structure studied by González Delgado et al. (1997a), other stellar indicators can be used for synthesis of very young populations in the FUV. The C III λ 1176 line and the P V λ 1118, 1128 doublet have been revealed, in fact, more powerful indicators than the O VI+Ly β +C II feature.

The new FUV library is a great opportunity to apply the spectral synthesis technique to various starbursts observed with FUSE. There are several advantages of the FUSE library on previous ones built in the same wavelength range or based on HST/UV and Copernicus data. First, the spectral resolution is exceptional and leads to more accurate diagnostics based on the detailed stellar line profiles. Second, ions of C III λ 1176 and P V λ 1118, 1128 do not show saturated profiles since C III is produced through excited atomic transitions and the P V doublet is of low cosmic abundance. This property allows a more accurate line profile fitting, especially at high metallicity, as it will be discussed in this work. Third, the flux calibration of FUSE data is more accurate than Copernicus data, which has some impact on the continuum normalization quality of the FUV stellar library. Fourth, the only stars contributing to $\lambda < 1200\text{\AA}$ are those hotter than 9200 K (\sim A0-A2 type). Consequently, the FUV is not contaminated by the flux from older underlying generation of stars. This will allow us to determine physical properties strictly related to young stellar populations.

The aim of this paper is to present FUV spectral synthesis on a relatively large sample of nearby starburst galaxies. For each FUV observation, we will obtain precise quantitative values of several fundamental physical parameters on the young stellar populations (i.e. age, metallicity, initial mass function, mode of star formation, stellar mass, and internal extinction). We first present in the next section, the extragalactic FUSE spectra and summarize the data processing. In §3 we briefly describe the `LavalSB` code and the FUV library. Results from the synthesis modeling for each individual galaxy are presented in §4. We conclude in section 5.

2 OBSERVATIONS AND DATA PROCESSING

The FUV spectra of the galaxies studied here have been taken from the FUSE archives through the *Multimission Archive at Space Telescope* (MAST¹). One exception is NGC 1667, for which A. Pellerin was the principal investigator. All FUSE spectra were collected with the $30'' \times 30''$ aperture (LWRS), except for NGC 5253 (MDRS), between 1999 and 2002. Table 1 summarizes the information relative to the galaxies and their observations. The six columns of the table give the galaxy's name, the morphological type and activity, the central coordinates for the exposures, the Galactic extinction from NED², the distance, the FUSE project data set identification, and the total exposure time. The FUSE data have been processed using the `calfuse` pipeline v2.2.2, the available version at that time. This version corrects for Doppler shift induced by the heliocentric motion of Earth, event bursts, the walk problem, gratings thermal shifts, bad

pixels, background noise, distortions, and astigmatism. More information relative to `calfuse` is available on the FUSE website³. Flux calibration is accurate to better than 10% in the LiF1A segment (between 987.1 and 1082.2 \AA) and the dispersion is about 15-20 km s⁻¹ pixel⁻¹.

Exposures obtained with the different detector segments have been combined in three steps. First, all exposures from the same segment have been added proportionally to their exposure time. Second, segments that cover the same wavelength range have been combined taking into account a statistical weight based on their signal-to-noise ratios (S/N). Note that a lower weight was given to the LiF1B segment (1094.3-1187.7 \AA) because of the flux default around 1145 \AA . This segment was not rejected because it covers the longer wavelength range where the stellar indicator C III λ 1176 can be located. In a third step, each wavelength range has been co-added to obtain a single spectrum.

A correction for astrophysical redshifts was also applied following the heliocentric radial velocities given by NED. Finally, the spectra were smoothed with a 20 pixels box using the task `boxcar` in IRAF⁴. This last operation increases the S/N without affecting the stellar line resolution needed for the spectral synthesis. The FUSE spectra presented in this work are electronically available on the MAST archives⁵.

3 EVOLUTIONARY SPECTRAL SYNTHESIS WITH LAVALSB

`LavalSB` is an evolutionary synthesis code for young stellar populations developed in parallel with `Starburst99` (Leitherer et al. 1999). A description of `LavalSB` in relation with its application to the synthesis in the FUV range can be found in Robert et al. (2003). In summary, `LavalSB` uses the evolutionary tracks of the Geneva group (Shaller et al. 1992; Schaerer, Meynet & Schaller 1993a; Schaerer et al. 1993b; Charbonnel et al. 1993; Meynet et al. 1994). Initially the stellar population obeys a mass distribution based on a chosen initial star formation scenario, i.e. an initial mass function (IMF) and mode of star formation (instantaneous or continuous). Individual stellar parameters are considered to assign the corresponding normalized empirical spectrum from the FUV library based on relations from Schmidt-Kaler (1982). The normalized library spectra are flux calibrated using stellar atmosphere models of Kurucz (1992) and of Schmutz, Leitherer, & Gruenwald (1992) for stars with extended envelop. Prior to their use, the Kurucz (1992) spectra have been fitted using a Legendre function in order to remove their low resolution spectral features. The code also includes evolutionary tracks for massive close binary stars, which was not used for the current work since binary stars do not have significant impact on UV line profiles (Dionne 1999; Dionne & Robert 2006).

The FUSE stellar library covers from 1003.1 to 1182.678 \AA with a dispersion of 0.127 \AA . For `LavalSB`, this library is composed of 155 Galactic stars from O3 to B3 spectral types, as well as 41 and 32 stars from the Large and Small Magellanic Clouds (LMC and SMC), respectively,

¹ <http://archive.stsci.edu/fuse/>

² NASA/IPAC Extragalactic Database; NED

³ <http://fuse.pha.jhu.edu/analysis/calfuse.html>

⁴ *Image Reduction and Analysis Facility*; <http://iraf.noao.edu/>

⁵ <http://archive.stsci.edu/prepds/fuse-galaxies/>

which includes spectral types between O3 and B0. Wolf-Rayet (WR) stars are also included. As pointed out by Robert et al. (2003), the lack of stars cooler than B0 at sub-solar metallicities produces a significant dilution of stellar line profiles for ages older than 7.0 Myr. The library metallicity is matched with the corresponding evolutionary tracks in `LavalSB`. For the LMC stars, we assume a metallicity of $0.4 Z_{\odot}$ (i.e. $12+\log[\text{O}/\text{H}]=8.3$, where the metallicity for solar environment objects corresponds to $12+\log[\text{O}/\text{H}]=8.7$). For SMC stars, we assume a metallicity around $0.2 Z_{\odot}$ (i.e. $12+\log[\text{O}/\text{H}]=8.0$). Evolutionary models at $2 Z_{\odot}$ are also produced with `LavalSB` but using the spectral library at solar metallicity. The reason is that not enough massive stars can be observed with FUSE with such a high metallicity. Below 1200\AA , the strength of stellar wind lines is significantly changing at high metallicity, unlike for $\lambda > 1200\text{\AA}$ where the profiles are quickly saturated. The consequences of using the solar metallicity library for objects with higher metallicity for FUV synthesis is not negligible and will be discussed in §4.

The work from Robert et al. (2003) has revealed that synthetic FUV spectra of young stellar populations contain important stellar indicators. The most useful ones are the C III multi-line centered at 1176\AA , and the P v doublet at 1118 and 1128\AA . The shape of these lines shows strong variations with age and metallicity. Significant, but more subtle, changes also appear with different IMF parameters. For young stellar population of less than ~ 10 Myr, at least, there is no age-metallicity degeneracy observed in the FUV; the age influence the global P Cygni profile while the metallicity mostly affects the line depth. At shorter wavelengths, the O VI $\lambda\lambda 1032, 1038$ and the S IV $\lambda\lambda 1063, 1073$ line profiles show variations with the age and metallicity, and possibly with the IMF. However, these diagnostic lines are contaminated by interstellar features of H_2 and other atomic transitions and are consequently more difficult to use for the spectral synthesis. Nevertheless, the C III $\lambda 1176$ and P v $\lambda\lambda 1118, 1128$ lines together are powerful indicators to find physical parameters of young stellar populations, as it will be shown in §4.

4 PROPERTIES OF YOUNG STELLAR POPULATIONS IN THE FUV

In this section, we present detailed results obtained from spectral synthesis for each individual starburst galaxy listed in Table 1. This work is part of Pellerin (2004, Ph.D. Thesis) where more details and figures can be found. The FUV synthesis is a three step process. First, for each normalized spectrum, the observed P v and C III line profiles are compared to various models produced with `LavalSB`. The models cover stellar populations with different IMF slopes (using mass cutoffs of 1 and $100 M_{\odot}$), and either instantaneous (where all stars are formed at the initial time) and continuous (where new stars are added to the population at each time step) modes of star formation. The comparison between the models and the normalized FUSE spectra is done both by eye and using a χ^2 method. In the case of noisy spectra, an eye judgment only is often unavoidable. This first step gives quantitative values, along with their uncertainties, for the age, the metallicity, and the IMF slope.

In a second step, the continuum level and its slope are studied. The spectra are first corrected for the Galactic reddening using the Cardelli, Clayton, & Mathis (1989) law. The internal extinction $E(B-V)_i$ for each starburst galaxy is evaluated from the FUV continuum slope using the theoretical extinction law from Witt & Gordon (2000) for a clumpy dust shell distribution with an optical depth of 1.5 in the V band. According to Buat et al. (2002), this law is in agreement with the observed FUV spectral energy distribution of starbursts. More precisely, the internal extinction is obtained by comparing the observed continuum slope β_{obs} (where $F_{\lambda} \propto \lambda^{\beta}$) with the synthetic slope β_{th} for the best model found from line profiles. The FUV slopes are measured through 5 small bandwidths that avoids stellar and major interstellar features (see Tab. 2). Also, we restricted these bands to the longer wavelengths of the FUSE spectrum since the continuum below 1200\AA is not always well represented by a power-law, especially at smaller wavelengths. We used the IRAF routine `curfit` with different values for the low and high pixel rejection levels to obtain an average value of the continuum slopes. Although this method gives uncertainties for the slopes, and therefore for the extinction, we also preformed a direct eye comparison of the galaxy extinction corrected spectrum with the synthetic spectrum. For galaxies with low signal-to-noise ratio spectra and those with a higher redshift (i.e. with limited spectral coverage at longer wavelength) larger uncertainty values for the extinction have been adopted, revealing still reasonable superposition of the spectra. Once a correction for the internal extinction is applied, the stellar mass M_{\star} involved in the observed burst is calculated. To do so, one must take into account the galaxy distance and then calculate the multiplying factor needed to superimpose the best-fitting synthetic spectrum obtained from the line profile to the flux level of the corrected spectrum. **Since the stellar mass is calculated after correction for internal extinction, the stellar mass value is highly dependent on the extinction evaluation, which depends strongly on the quality of the spectra and its spectral interval coverage. As it will be discussed later in the text, the stellar mass values derived from FUV luminosities are usually in good agreement with other works, but can lead to large uncertainties (and nonsense values) when the spectra quality is poorer. For example, an error of 0.1 in $E(B-V)$ will lead to a variation of $\text{Log}(M_{\star})$ of ± 1 .**

The third step uses `LavalSB` to compute and predict other galaxy observables based on the best-fitting model. We compute the flux and equivalent width (EW) of the nebular line $\text{H}\alpha$, the number of O, B, and WR stars, the flux of the WR bump around 4686\AA , and the continuum flux level at 5500\AA . These predictions are then compared to observations found in the literature. Taking into account the different apertures used, such comparisons often offer a good test for the FUV synthesis.

In the following sub-sections, we first discuss the case of well-known starburst galaxies for which we can compare the FUV synthesis results with analysis at other wavelengths from the literature. In §4.2, we discuss the impact of discrete metallicity values available in the code on integrated stellar populations with an intermediate metallicity. We then perform, in §4.3, the FUV synthesis of relatively low metallicity

objects and discuss the limitation of the FUV library. In §4.4 we present the case of stellar populations for which a non-standard IMF slope has been obtained. The FUV synthesis of low signal-to-noise ratio spectra is described in §4.5. Finally, in §4.6 and §4.7, we summarize the synthesis result for Seyfert galaxies, some of which showing a FUV spectrum dominated by a young stellar population and others dominated by their non-thermal emission.

4.1 FUV Synthesis of Well-Known Galaxies:

NGC 7714 is a spiral galaxy often described as the prototype for nuclear starbursts (Weedman et al. 1981; González Delgado et al. 1999). The FUSE aperture is centered on the nuclear region, covering a field of $5.7 \times 5.7 \text{ kpc}^2$ (at a distance of 37.5 Mpc; see Table 1). Figure 1 shows the good quality spectrum of NGC 7714 obtained by FUSE (with $S/N \simeq 15$ at 1150 \AA). The diagnostic line of C III displays a strong photospheric profile as well as a weak but broad absorption in the blue wing which is an indication of stellar wind from O-type stars. The P v doublet shows deep and well-defined absorptions. The best model for the P v and C III line profiles, as shown in Figure 1, is obtained for an instantaneous burst of $4.5 \pm 0.3 \text{ Myr}$ at solar metallicity, and using a standard IMF ($\alpha = 2.35$, from 1 to $100 M_{\odot}$). Models with an age of 4.0 and 5.0 Myr are significantly less satisfying to reproduce the line profiles. Models with another metallicity do not give the right depth for the lines. Note that a different IMF slope between $\alpha = 2.2$ and 3.3, can also fit the data, but because of the spectrum noise level, we simply adopt here a standard IMF for our study. A continuous burst of $\sim 10\text{-}20 \text{ Myr}$ can also reproduce the line profile, but one must be careful in this specific case before concluding. Indeed there is a degeneracy between some continuous burst models and an instantaneous burst of $\sim 4.5 \text{ Myr}$. This effect is not seen for an instantaneous burst at a different age. For other galaxies of our sample having a different age and enough signal in their FUSE spectrograms, the case of a continuous burst is generally discarded. For this reason, we favor the instantaneous model for NGC 7714. The best model parameters retained from the FUV synthesis are reported in Table 3.

An age of 4.5 Myr is in agreement with previous studies using other wavelength bands (González Delgado et al. 1999; García-Vargas et al. 1997; González Delgado et al. 1995). An ambiguous point in the literature is the metallicity of NGC 7714. González Delgado et al. (1995) measured $12 + \log[\text{O}/\text{H}] = 8.5$ (i.e. $0.6 Z_{\odot}$) for the nucleus, while Heckman et al. (1998) compiled from other papers an oxygen abundance higher than solar. More recently, Fernandes et al. (2004) obtained $12 + \log[\text{O}/\text{H}] = 7.9$ (i.e. $0.2 Z_{\odot}$). The limited precision in metallicity of LavalSB do not allow us to distinguish between the values of González Delgado et al. (1995) and Heckman et al. (1998), but certainly the FUSE synthesis do not agree with the metallicity of Fernandes et al. (2004).

Based on the best-fitting model for the line profiles, the FUV continuum slope should be $\beta_{th} = -1.8 \pm 0.2$. A comparison with the FUSE spectra allow us to estimate an internal extinction $E(B-V)_i = 0.1 \pm 0.1$, if we consider a Galactic contribution $E(B-V)_{Gal} = 0.08$, as proposed by González Delgado et al. (1999). The UV continuum slope

and the flux level at 1150 \AA , after correction for the Galactic extinction, are given in Table 3. This is consistent with result of 0.03 obtained from HST/GHRS spectra by González Delgado et al. (1999). One important difference with this study is the aperture size; the HST/GHRS aperture is $1.74'' \times 1.74''$ which is much smaller than the FUSE aperture.

When correcting the FUSE spectrum with the internal extinction of $E(B-V)_i = 0.1$, we estimate that the total stellar mass responsible for the observed FUV flux is of the order of $10^8 M_{\odot}$. The mass uncertainty is mainly related to the extinction uncertainties. These results are consistent with a mass of $6.8 \times 10^7 M_{\odot}$, derived by González Delgado et al. (1995) from the $\text{H}\alpha$ intensity ($1.2''$ slit), and $1.1 \times 10^8 M_{\odot}$, from González Delgado et al. (1999) based on the IUE ($10'' \times 20''$) flux observed at 1500 \AA . The mass differences can be easily explained by the various internal extinctions and aperture sizes used.

Using the starburst physical parameters found from the FUV synthesis, it is possible to predict several features in the visible range. Table 4 gives, for example, the number of O stars and the WR/O ratio obtained from the best model, along with the predicted flux and EW for the $\text{H}\alpha$ line, the equivalent width of the WR bump at 4686 \AA , and the continuum flux level at 5500 \AA . In the central 330 pc ($1.74''$) of NGC 7714, González Delgado et al. (1999) derived about 16 600 O stars. The best model for the FUSE data predicts 12 times more O stars within the central $30'' \times 30''$. The large difference in aperture sizes do not allow us to compare these numbers. The same authors derived a WR/O ratio of 0.12, relatively close to the ratio of 0.19 derived with FUSE. Note that this last ratio is very sensitive to the age, i.e. at 5.0 Myr LavalSB gives 0.12. González Delgado et al. (1995) also detected a WR bump in a $1.2''$ slit with $\text{EW}(4686) = 1 \text{ \AA}$, a much lower value than 44 \AA as predicted for the FUSE aperture. The $\text{H}\alpha$ flux and equivalent width of NGC 7714 have been measured by several authors. If we limit our comparison with the $1.9 \times 10^{-12} \text{ ergs s}^{-1} \text{ cm}^{-2} \text{ \AA}^{-1}$ $\text{H}\alpha$ flux value of Storchi-Bergmann, Kinney & Challis (1995) in a large $10'' \times 20''$ aperture, the value predicted from the FUV is very consistent. Storchi-Bergmann et al. (1995) also measured a continuum flux $F(5550) = 1.4 \times 10^{-14} \text{ ergs s}^{-1} \text{ cm}^{-2} \text{ \AA}^{-1}$, which corresponds well again to the FUSE prediction of $10^{-14} \text{ ergs s}^{-1} \text{ cm}^{-2} \text{ \AA}^{-1}$.

IRAS 08339+6517 is a spiral galaxy with a strong and compact nuclear starburst (Margon et al. 1988) which was probably triggered by an interaction with 2MASX J08380769+6508579 (Cannon et al. 2004). Because of its relatively large distance (78 Mpc), the C III structure is redshifted outside the FUSE spectral range, as seen in Figure 1. The high S/N of ~ 15 allows a good synthesis of the P v doublet. From the P v line profiles, we find an age of $7.0 \pm 0.3 \text{ Myr}$ for an instantaneous burst at Z_{\odot} . A standard IMF is adopted, but a good fit is also obtained for an IMF slope of 2.8. A continuous burst cannot reproduce the line profiles since this scenario would always show P Cygni profiles in P v, which are not observed in IRAS 08339+6517. The age and metallicity from the FUV synthesis are in really good agreement with the previous work of Margon et al. (1988) in the visible, González Delgado et al. (1998a) and Leitherer et al. (2002a) using UV spectra from HUT and

HST, and Pellerin (1999) with visible and near-infrared spectra.

Using our best-fitting model for the FUV line profiles, we calculate an internal extinction $E(B-V)_i=0.30\pm 0.15$, with $E(B-V)_{Gal}=0.092$ (NED). The large uncertainty comes from the fact that the rest-frame FUV spectrum is incomplete at longer wavelength due to the relatively high redshift of IRAS 08339+6517. A stellar mass of 10^8 to $10^{12} M_\odot$ is then derived for the young burst. **We can see here the effect of the shorter spectral coverage on the mass estimate, which lead to large uncertainties. A mass of 10^{11} - $10^{12} M_\odot$ is similar to the mass of an entire spiral galaxy like the Milky Way. Such a mass is clearly unreasonable in the case of IRAS 08339+6517 since the FUSE aperture does not even cover the full galaxy. The stellar mass values are obviously less reliable when the uncertainties on extinction increase.** González Delgado et al. (1998a) and Leitherer et al. (2002a) obtained $E(B-V)_i=0.17$ from the HUT data (using $E(B-V)_{Gal}=0.08$, which is similar to the value we used). Their internal extinction is fairly consistent within the lower limit of the value obtained from the FUV. **For this reason, we suspect that the stellar mass for the nuclear starburst in IRAS 08339+6517 is probably closer to $10^8 M_\odot$.**

Predicted values for visible features for IRAS 08339+6517 are reported in Table 4. Margon et al. (1988, with a $22''$ diameter aperture), González Delgado et al. (1998a, $10''\times 20''$ aperture), and Pellerin (1999, $4''$ slit) observed an $H\alpha$ flux of 0.7, 1.3, and 1.5×10^{-12} ergs $s^{-1} cm^{-2} \text{ \AA}^{-1}$, respectively. These are low compared to the predicted value of 10^{-10} ergs $s^{-1} cm^{-2} \text{ \AA}^{-1}$, but in agreement considering the large uncertainties. The flux level at 5500\AA observed by Pellerin (1999) is 1.8×10^{-14} ergs $s^{-1} cm^{-2} \text{ \AA}^{-1}$, consistent within the lower limit predicted from FUSE data. It may also indicate that FUSE, with its larger aperture, is seeing more than just a central compact starburst.

M 83 (NGC 5236) is a well studied spiral galaxy at a distance of 3.8 Mpc. The FUSE aperture covered the circumnuclear ring of star formation. In Figure 1, the observed C III line clearly displays a broad absorption in its blue wing, which is associated with evolved O stars. The important depth of C III and P v suggests metal rich stars. While LavalSB has evolutionary tracks at $2Z_\odot$, it does not have a stellar library at this metallicity (see §3). Nevertheless, a relatively good fit at $2Z_\odot$ is found, which can satisfy the width and the emission part of the P Cygni profiles for an age of 3.5 ± 0.5 Myr. As shown in Figure 1, the line depth cannot be reproduced because of the lack of metal rich stars in the FUV library. However, we can assert that the metallicity is significantly higher than solar. A standard IMF was simply adopted here because of the impossibility to properly consider the line depth. A continuous burst model cannot be adjusted to the FUSE spectrum of M 83 mainly because the synthetic P v doublet shows P Cygni profiles which are too weak compared to the observed lines.

The age obtained from the FUV synthesis is in good agreement with other observations (Elmegreen, Chromey & Warren 1998; Puxley, Doyon & Ward 1997; Harris et al. 2001; Leitherer et al. 2002a). In their detailed work,

Bresolin & Kennicutt (2002) studied individual knots of star formation around the galaxy center. The brightest and youngest knot, named A, displays a 4 Myr old population with evidence for WR stars. It seems therefore that knot A contributes significantly to the FUSE spectrum. The high metallicity obtained from the FUV is consistent with the work of Zaritsky, Kennicutt & Huchra (1994) and Bresolin & Kennicutt (2002) who found an oxygen abundance of $12+\log[O/H]=9.2$ (i.e. $3.2Z_\odot$).

From the FUV continuum slope, we measure an intrinsic extinction $E(B-V)_i=0.08\pm 0.08$, using $E(B-V)_{Gal}=0.066$ (NED). From the Balmer decrement, Storchi-Bergmann, Calzetti & Kinney (1994) and Calzetti et al. (1995) measured a total extinction of 0.29, consistent with the FUV extinction. Although the aperture sizes are quite different, it is normal to find a UV extinction that is lower by 50% compared to the extinction from the Balmer decrement (Calzetti et al. 1995). After corrections for the reddening, the FUV flux gives a stellar mass between 2.5×10^5 and $10^7 M_\odot$. The work of Bresolin & Kennicutt (2002) revealed a stellar mass of $\sim 10^5 M_\odot$ for knot A only, which strongly suggests again that it is a major contributor to the observed FUSE spectrum.

Bresolin & Kennicutt (2002) also studied the WR content in M 83. For knot A, they measured $EW(4686)=4.6\text{\AA}$ from which they estimated the presence of 31 WR stars. LavalSB predicts $EW(4686)=18\text{\AA}$ and about 2000 WR stars (see Tab. 4). This discrepancy can easily be explained by the fact that the FUSE aperture includes other young knots and also because the WR bump at 4686\AA can underestimate the number of WR stars due to the contribution of other stellar populations to the visible continuum (Chandar, Leitherer, & Tremonti 2004). Crowther et al. (2004) identified 1030 WR stars for the whole galaxy, and this number might reach 1500, according to their prediction. FUV synthesis results are consistent with their observations, considering the large uncertainty of the predicted values and the very different apertures.

Bresolin (2003; private communication) measured $F(H\alpha)=1.34\times 10^{-12}$ ergs $s^{-1} cm^{-2} \text{ \AA}^{-1}$ and $F(5500)=6.94\times 10^{-15}$ ergs $s^{-1} cm^{-2} \text{ \AA}^{-1}$ for knot A alone, yet showing the importance of this knot to the luminosity in the nuclear region based on the FUV predictions (see Tab. 4). Storchi-Bergmann et al. (1995), using a $10''\times 20''$ aperture, measured an $H\alpha$ flux which is 10 times smaller than the one predicted by LavalSB. On the contrary, Storchi-Bergmann et al. (1995) measured a continuum flux at 5500\AA which is twice as strong as the one predicted from the FUV. This suggests that there is an important contribution to the visible continuum flux from an older stellar populations (too cold to be seen in the FUV) which is diluting the $H\alpha$ line flux.

NGC 3690 (Mrk 171) is a member of the highly perturbed interacting system Arp 299 (Hibbard & Yun 1999). NGC 3690 and its companion, IC 694, are both displaying intense starbursts. The FUSE aperture includes most the emission from NGC 3690 and excludes IC 694. As shown in Figure 1, the FUV spectrum displays an incomplete C III line. Nevertheless, the blue wing of the C III line is still very useful for a FUV synthesis. Models for an instantaneous burst at solar metallicity are best to reproduce the C III and P v line depths. While the C III line favors models with an

age between 5.5 and 6.5 Myr, the P v feature is better adjusted by a burst of 6.5-7.0 Myr. The best-fitting model of 6.5 ± 0.5 Myr also indicate a standard IMF. For example, a steeper IMF slope is rejected because it cannot reproduce the weak blue wing observed for the C III line.

From visible and IR data, ages between 3.5 and 8 Myr have been found for individual bright knots in NGC 3690 (e.g. Gehrz, Sramek & Weedman 1983; Bonatto et al. 1999; Satyapal et al. 1999; Alonso-Herrero et al. 2000). Schaefer, Contini & Pindao (1999) detected WR star signatures in a region inside the FUSE aperture which also indicates a young age. Robert (1999) performed the UV synthesis of a HST/FOS spectrum obtained with a $1''$ aperture centered on knot B2 (included in the FUSE aperture) and found an age of 6.5 Myr. A metallicity of $1.26 Z_{\odot}$ was measured by Heckman et al. (1998) which is also consistent with the FUV result.

Using the best model above, we measured an internal extinction $E(B-V)_i = 0.15 \pm 0.05$, when adopting $E(B-V)_{Gal} = 0.017$ (NED). After correction for the extinction, the FUV flux level gives a stellar mass of $10^8 M_{\odot}$ for the young burst. Alonso-Herrero et al. (2000) estimated a mass of $3 \times 10^7 M_{\odot}$ for the small knot B2 alone. Table 4 reports values of the visible flux and line equivalent widths predicted from the FUV synthesis. Although generally consistent with the literature, these numbers must be compared with caution mainly because they have been collected using a different aperture size. For example, Gehrz et al. (1983) used a small $4''$ slit and measured a value for the $H\alpha$ flux which is 5 times weaker than the one predicted. Kennicutt (1992) found a closer number with a circular aperture of $45''$ diameter. Alonso-Herrero et al. (2000) and Friedman et al. (1987) gave $H\alpha$ equivalent width measurements between 55 and 600 \AA for various knots, which brackets the FUSE prediction of $140_{-120}^{+180} \text{ \AA}$.

NGC 3310 has a very blue compact nucleus and a circumnuclear starburst. The FUSE aperture contains both structures and allows us to study most of the galaxy star formation activity since it is estimated to take place within the central $20''$ (Smith et al. 1996). Figure 1 shows a high quality FUV spectrum for NGC 3310 with a $S/N \simeq 20$. Note that the stellar P v $\lambda 1118$ line is contaminated by Galactic interstellar lines of H_2 . The P v $\lambda 1128$ component and the C III line do not show any extended blue absorption from stellar wind. From this, we conclude that no significant O star population is present. We find that the best line profile adjustment is obtained with an instantaneous burst of 18 ± 2 Myr at $2 Z_{\odot}$ and a standard IMF. Another model can reasonably fit the lines, which consists of a 15 ± 1 Myr burst at Z_{\odot} , if a steeper IMF slope of 2.80 is used. It would probably be possible to separate the two cases if a proper stellar library at $2 Z_{\odot}$ was available. An abundance of $12 + \log[O/H] = 8.8-9.0$, corresponding to $1.3-2.0 Z_{\odot}$ was found by Heckman et al. (Denicoló, Terlevich & Terlevich 2002 and 1998). This favors the model at $2 Z_{\odot}$. Furthermore, no continuous burst model can reproduce the observations.

Only a few studies addressing the stellar content in the nucleus of NGC 3310 are found in the literature. Most suggest an age between 6 and 20 Myr (Boisson et al. 2000; Leitherer et al. 2002a; Elmegreen et al. 2002; Hugues et al. 2005). However, Pastoriza et al. (1993) found a younger age for a small region located about $10''$ (SW) from the nucleus,

based on the observation of a WR bump at 4686 \AA . However, the FUSE spectrum do not show evidence of a stellar population younger than 10 Myr probably because these young stars do not contribute significantly to the FUV flux within the large aperture. These stars seem to be completely diluted by a more important B-type star population.

Considering the best-fitting model at $2 Z_{\odot}$, we estimate an internal extinction $E(B-V)_i = 0.05 \pm 0.05$ (using $E(B-V)_{Gal} = 0.022$) and a stellar mass of $0.39-3.9 \times 10^8 M_{\odot}$. The stellar mass of $2.2-8.4 \times 10^8 M_{\odot}$ calculated by Smith et al. (1996) within a $\sim 25''$ inner region is in agreement with FUV result. Table 4 reports the predicted fluxes and EW in the visible for NGC 3310. Pastoriza et al. (1993) measured a continuum flux levels at 5510 \AA for individual regions. If we add together their fluxes for the seven knots included within the FUSE aperture, we obtain a lower limit of $F(5500) > 1.5 \times 10^{-14} \text{ ergs s}^{-1} \text{ cm}^{-2} \text{ \AA}^{-1}$, which is consistent with the synthetic flux between 2.5 to $25 \times 10^{-14} \text{ ergs s}^{-1} \text{ cm}^{-2} \text{ \AA}^{-1}$. However, the predicted flux for $H\alpha$ is significantly lower than the $1.4 \times 10^{-12} \text{ ergs s}^{-1} \text{ cm}^{-2} \text{ \AA}^{-1}$ measured by Pastoriza et al. (1993) for the same seven knots, suggesting a contribution to $H\alpha$ from other sources not seen in the FUV.

4.2 Adjusting the Metallicity

NGC 4214 is a relatively close (3.4 Mpc) irregular galaxy with many knots of intense star formation. Doing the FUV synthesis of its FUSE spectrum (shown in Fig. 2) was not easy at first. Despite a high S/N of ~ 19 , we were unable to obtain an adequate adjustment of the stellar lines using the models at the available metallicities. Mainly, models at $0.4 Z_{\odot}$ produce stellar lines which are too shallow while lines from models at Z_{\odot} are too deep. Among these, the best model (but still not satisfying) was obtained for an instantaneous burst of 4.5-5.0 Myr at $0.4 Z_{\odot}$ with $\alpha(\text{IMF}) \leq 2.35$.

Kobulnicky & Skillman (1996) report an abundance $12 + \log[O/H] = 8.2$ (i.e. $0.3 Z_{\odot}$) for NGC 4214, which is consistent with a modeling at low metallicity. Furthermore, these authors observed an abundance gradient. Considering this spatial variation and the existence of multiple knots of star formation, we then performed a more sophisticated synthesis. We compared the observed FUV spectrum with the synthetic spectrum of a double burst model. This model was created by combining two synthetic spectra of two different bursts, one at a metallicity of $0.4 Z_{\odot}$, and the other at Z_{\odot} . A standard IMF was assumed here. The comparison of the observed spectrum with those obtained with the double bursts model are shown in Figure 3. The P v and C III line profiles are better reproduced if we consider an age of 5.5 Myr and a similar flux proportion for the two bursts. Models of 5.0 and 6.0 Myr have more difficulty to reproduce the blue wing of C III, but still give reasonable fits. Other flux proportions between the two bursts are less good at reproducing the line profiles. In conclusion, the global metallicity for the stellar population seen with FUSE in NGC 4214 seems to be slightly higher than the LMC metallicity. A detailed study of the stellar content of NGC 4214 has been performed by Leitherer et al. (1996), revealing around 200 point sources, apparently individual hot stars of small clusters, distributed around a more important starburst. Their UV synthesis based on an HST/FOS spectrum ($1''$ circular

aperture) on the central burst leads to an age of 4-5 Myr, which is in good agreement with our results.

The spectral energy distribution of NGC 4214 shows some fluctuations. This problem was also observed for NGC 5253 (from the same observing program) and Mrk 153. Compared to the synthetic energy distribution, the continuum level at $\lambda > 1100\text{\AA}$ is too high, and the level between 1000 and 1100 \AA is too low (not shown here). This behavior cannot be attributed to the stellar population itself or the ISM. It is possibly related to the alignment of the FUSE spectrograph optical paths. If this alignment is not perfect, especially for extended targets, the flux can be slightly different from one segment to another, as seen here. The consequence is to increase the uncertainties on the extinction and the stellar mass.

Despite these fluctuations, we estimate an internal extinction of 0.13 ± 0.03 using a $E(B-V)_{Gal} = 0.022$ (NED), which is in agreement with the measurement of Leitherer et al. (1996). This leads to a stellar mass of $(2 \pm 2) \times 10^6 M_{\odot}$ for the young burst. Predicted fluxes and EW for H α and continuum observables (Tab. 4) are in good agreement with the observations of MacKenty et al. (2000, using a 40'' diameter aperture). Sargent & Filippenko (1991) observed WR bumps in 4 bright knots and estimated that about 233 WR star were present in those knots. This is only 25% of the value predicted by LavalSB for a 5.5 Myr population. The difference suggests that an important number of WR stars resides in other clusters.

NGC 5253 is experiencing a violent star formation event possibly due to its interaction with M 83 (Calzetti et al. 1999). As shown in Figure 2, the C III and P v lines in the FUSE spectrum of NGC 5253 and NGC 4214 are quite similar, showing the same line depth and no P Cygni profile. The synthesis is again indicating an age of ~ 4.5 Myr, with a metallicity around $0.4 Z_{\odot}$, but the result is not fully satisfying. The difficulty encountered here is identical to the one for NGC 4214 and probably has the same origin since both objects have a similar metallicity (Denicoló et al. 2002). Therefore, we are considering synthetic spectra which are composed of a blend of two models with metallicities of $0.4 Z_{\odot}$ and Z_{\odot} . Our best synthetic spectrum (see Fig. 4) indicates, assuming a standard IMF, a flux proportion of about 75% for the $0.4 Z_{\odot}$ population and about 25% for the Z_{\odot} population, with an age of 5.5 ± 1.0 Myr for both populations. In conclusion, we estimate that the global stellar population of NGC 5253 is well represented with a metallicity between 0.4 and $0.5 Z_{\odot}$. This idea of an intermediate metallicity was also raised by Tremonti et al. (2001) while analyzing visible data with **Starburst99**. This age found is consistent with previous works (Calzetti et al. 1997; Tremonti et al. 2001). Leitherer et al. (2002a) estimate an average age of 20 Myr with HUT spectra and a $10'' \times 56''$ aperture, and they assert that O stars, while present, are not dominant in this object, which is different from the FUV point of view.

Using the Galactic extinction values of 0.056 (NED), we find an internal extinction of 0.05 ± 0.05 . With this correction, we estimate a stellar mass of 0.8 to $7.9 \times 10^5 M_{\odot}$. The uncertainty for the stellar mass also takes into account the problem seen for the flux distribution, as discussed for NGC 4214. A value of $6.6 \times 10^4 M_{\odot}$ was obtained by Tremonti et al. (2001) using a long slit, while a mass of $10^5 M_{\odot}$ was calculated by Calzetti et al. (1997) for the five

brightest knots together. These values are consistent with each other, considering differences in apertures and extinction values.

The continuum level at 5500\AA obtained by Storchi-Bergmann et al. (1995), with a $10'' \times 20''$ aperture, is of $2.4 \times 10^{-14} \text{ ergs s}^{-1} \text{ cm}^{-2} \text{ \AA}^{-1}$. This is consistent with the predictions (see Tab. 4). The predicted H α flux is also in agreement with the value of 7.7×10^{-12} from Calzetti et al. (1997) for the five brightest clusters included within the FUSE aperture. It is interesting to note that that the brightest knot (#5) alone produces an H α flux of $5.8 \times 10^{-13} \text{ ergs s}^{-1} \text{ cm}^{-2} \text{ \AA}^{-1}$. This knot has a 0.35 mag of internal absorption between H α and H β , which certainly leads to a strong obscuration of this knot at UV wavelengths. Schaerer et al. (1997) estimated the number of hot stars in NGC 5253. They obtained 1730 and 840 O stars in their region A and B, respectively, and a WR/O ratio of 0.02 and 0.06 for the same two regions. The number of O-type stars consistent with the predicted values of LavalSB, while the number of WR stars is very sensitive to the age of the best model.

4.3 Low Metallicity Starbursts and the Limit of the FUV Library

Mrk 153, although less studied, is a well established starburst galaxy. Its FUV spectrum is of good quality, with $S/N \simeq 19$ at 1150\AA , except in the LiF1B segment around the C III line where it becomes more noisy (see Fig. 5). Its P v and C III lines are similar to those of NGC 4214 and NGC 5253 (Fig. 2) with no sign of wind profiles (i.e. extended blue wings). Note that the P v $\lambda 1118$ component is possibly contaminated by an airglow line. Shallow stellar lines are usually an indication of a metal poor population. Based mainly on the P v $\lambda 1128$ feature, a good model might be an instantaneous burst of 6.5 ± 1.0 Myr at $0.2 Z_{\odot}$, assuming a standard IMF. A model at $0.4 Z_{\odot}$ is rejected as it produces absorption lines in P v that are too deep. However, as shown in Figure 5, the best model cannot reproduce the depth of the C III feature. Although the S/N is lower in this wavelength range, we believe it is an indication of an older age for the burst. Around this age, synthesis work at low metallicity is limited by the fact that stars cooler than B0 are missing in the spectral library (see §3). Because of this limitation, we did not test other IMF slopes. Kunth & Joubert (1985) have found a metallicity of $0.1 Z_{\odot}$, i.e. 7.8 in $12 + \log[\text{O}/\text{H}]$. Also, based on an IUE spectrum, Bonatto et al. (1999) conclude to an age < 10 Myr. These results are consistent with the FUV synthesis.

Based on the FUV slope for a 6.5 Myr old stellar population, we calculate an intrinsic extinction of 0.07 ± 0.07 , with $E(B-V)_{Gal} = 0.013$. The stellar mass associated to the FUV flux is then 0.25 - $10 \times 10^7 M_{\odot}$. Predicted properties based on the best FUV model for Mrk 153 are listed in Table 4. Mazzarella & Boroson (1993) have measured the H α flux in a narrow $1''$ slit. They obtained $9.9 \times 10^{-14} \text{ ergs s}^{-1} \text{ cm}^{-2} \text{ \AA}^{-1}$ in total for a group of clusters. This is larger than the value of 0.16 - $2.5 \times 10^{-14} \text{ ergs s}^{-1} \text{ cm}^{-2} \text{ \AA}^{-1}$ predicted for the large FUSE aperture which includes these clusters.

IZw 18 is a blue compact dwarf (BCD) well known for its very low metallicity (e.g. Thuan 1983; Kunth, Matteucci & Marconi 1995; Hunter & Thronson

1995; Izotov et al. 1997). A review of this particular object was presented by Kunth & Östlin (2000). The FUSE spectrum of IZw 18 is shown in Figure 5 with a good S/N of ~ 18 . The stellar lines show no sign of wind profiles and they are rather faint, suggesting a relatively old and/or metal-poor stellar population. A synthetic spectrum for an instantaneous burst of 7.0 Myr at $0.2 Z_{\odot}$ is superimposed on the FUSE spectrum in Figure 5. The age of 7 Myr is the lower limit imposed by the lack of stars cooler than B0 in our spectral library at $0.2 Z_{\odot}$ (see §3). With this limitation, we simply adopted an IMF with $\alpha=2.2$, as suggested by Aloisi, Tosi & Greggio (1999). As shown in Figure 5, the model does not reproduce well either the P v or C III line strengths. It is suspected that an older model of 10-20 Myr, as found by Aloisi et al. (1999) and Östlin (2000), would not show significant change in the line strengths. However, a lower metallicity model is likely to produce weaker lines. This would be consistent with the very low metallicity estimated for IZw 18 (e.g. Dufour, Garnett & Shields 1988; Izotov et al. 1999; Aloisi et al. 2003).

Adopting a model of 15 Myr with $\alpha=2.2$ at $0.2 Z_{\odot}$, we can roughly estimate some physical parameters for IZw 18 from the measured FUV flux level. We obtain $E(B-V)_i=0.0$ if the Galactic extinction is 0.032 (NED). This low internal extinction is compatible with other values found in the literature (e.g. Aloisi et al. 1999; Cannon et al. 2002) using optical data. Correcting the FUSE spectrum with this extinction, we obtain a stellar mass of 10^6 - $10^7 M_{\odot}$ for the young burst while Kunth & Östlin (2000) estimate it to $5 \times 10^6 M_{\odot}$ from optical imaging with a similar aperture.

In general, the fluxes calculated by `Lava1SB` are in reasonably good agreement with observations considering the various aperture sizes (Izotov et al. 1997; Pagel et al. 1992). Nevertheless, some studies show clear indications of very young stars in a few clusters. For example, Izotov et al. (1997) detected a weak WR signature in an isolated knot (1.5'' slit) for which they estimated 1100 O stars and 22 WR stars. Mas-Hesse & Kunth (1999) also calculated a WR/O ratio of 0.0003. Pagel et al. (1992) measured a larger $EW(H\alpha)$ of 518 and 1218 \AA for the two brightest knots, which is much higher than the value predicted from the FUSE data. With the large aperture used with FUSE, it is likely that the flux from small events is quickly diluted by the dominant 15 Myr old stellar population for which O and WR stars are not predicted.

NGC 1705 is an irregular BCD galaxy relatively well studied because of its proximity. The LWRS/FUSE aperture was used to obtain a FUV spectrogram with $S/N \approx 20$ (see Fig. 5) for the central $744 \times 744 \text{ pc}^2$. From the line depths, we conclude that the metallicity is around $0.4 Z_{\odot}$. The absence of wind profile in the C III feature indicates a population dominated by B-type stars. Again, as it was the case for IZw 18, the synthesis of NGC 1705 is limited by the lack of B-type stars in the spectral library at sub-solar metallicities (see §3) and we can only conclude that the age of this stellar population is older than 7 Myr (see Fig. 5). This is consistent with the study of Vázquez et al. (2004) where they derived an age of 12^{+3}_{-1} Myr for the brightest super-star cluster (NGC 1705-1) using HST/STIS. This also suggests that NGC 1705-1 may be an important contributor to the UV flux. Tosi et al. (2001) resolved several individual stars using HST/WFPC2+NICMOS data and concluded that

the youngest burst is 10-20 Myr old. Heckman & Leitherer (1997) arrived at the same result with HST/GHRS data. (Storchi-Bergmann et al. 1994) also found a low metallicity of $0.46 Z_{\odot}$ for NGC 1705.

Adopting a 15 Myr instantaneous burst at $0.4 Z_{\odot}$ with a standard IMF, we find $E(B-V)_i=0.01 \pm 0.01$ for a Galactic extinction of 0.008 (NED), and a stellar mass of 2.0 - $3.2 \times 10^6 M_{\odot}$. Along with the model predictions given in Table 4, these are rough estimates as we are considering an approximate model for the lines. Nevertheless, the predicted flux at 5500 \AA is in good agreement with the observation of Storchi-Bergmann et al. (1995). However, the $H\alpha$ flux of $4.3 \times 10^{-13} \text{ ergs s}^{-1} \text{ cm}^{-2} \text{ \AA}^{-1}$ measured by these authors, through a $10'' \times 10''$ aperture, is a factor of 5-10 higher than the FUV prediction. Annibali et al. (2003) have isolated a 2-3 Myr old population in the central 100 pc. This isolated population is possibly responsible for the large $H\alpha$ flux, but its FUV flux is obviously diluted in a large aperture.

4.4 Non-Standard IMF or Bursts Superposition

NGC 4449 is an irregular galaxy with a large number of young star clusters (e.g. Gelatt, Hunter & Gallagher 2001; Böker et al. 2001). FUSE obtained data for two different regions in NGC 4449, one centered on the nucleus and the other on an H II region located South-West from the nucleus. The FUV stellar lines seen (Fig. 6) for the nuclear region are better reproduced with an instantaneous burst of 10 ± 1 Myr at Z_{\odot} . No continuous burst model can fit the observations. An IMF slope of 3.3 is required, especially for the C III structure. A 8 Myr burst with $\alpha=2.8$ is slightly better for the P v line profiles, but gives unsatisfying results for the C III feature. The H II region spectrum is relatively well reproduced by a 5.0 ± 0.5 Myr burst at Z_{\odot} . As for the nuclear region, a steep IMF with $\alpha=3.3$ offers the best compromise for the C III and P v lines.

The fact that we are clearly finding a steep IMF slope for this galaxy may be surprising at first since this object is known to display a standard IMF (e.g. Massey 1998; Kroupa 2004). However, the IMF slope given by the FUV line synthesis may be interpreted in other ways than a real steep IMF for the massive stars. An hypothesis to explain a steep IMF and the problem related to P v line profile fitting would be the contribution of an older stellar population dominated by B-type stars. The FUV range ($900 \text{ \AA} < \lambda < 1200 \text{ \AA}$) is particularly sensitive to the relative number of O and B stars since they are the only stars to produce photons below 1200 \AA . Considering this fact, if an important population dominated by B stars is superposed, in the right proportion, to a younger burst, it will increase the total number of B stars seen in the FUV range and then modify the global IMF slope. This would explain the steep IMF without referring to some peculiar star formation processes.

To test the hypothesis of a stellar population superposition, we combined synthetic spectra of two stellar populations with the same IMF slope of 2.35, but having different ages and various flux proportions. These new models have been compared to the single population with $\alpha=3.3$, as observed in NGC 4449. Results are reported in Figure 7 for young instantaneous bursts of 10 and 5 Myr (for the nuclear and the H II regions respectively), both combined with an

older burst of 20 Myr. It shows that the line profiles of the young burst are, as expected, diluted by a B star population of 20 Myr. If 25 to 50% of the total stellar flux contributing to the light comes from the 20 Myr burst, the FUV line profiles then correspond well to the one of a single young burst with $\alpha=3.3$. From this, we conclude that the FUSE spectra of NGC 4449 are produced by more than one important stellar population, each with a standard IMF. This conclusion reinforces the results of Gelatt et al. (2001) who claimed that an active star formation took place in NGC 4449 during the last 10 Myr to 1 Gyr.

We also considered the time-dependent dust obscuration effect as proposed by Leitherer, Calzetti, & Martins (2002b). In this particular case, the contribution of dust being less pronounced, if not absent, around older stars, one can expect to observe more B-type than O-type stars. Following these authors, the time-dependent dust obscuration effect can be mixed up with a steep IMF. But for this effect to be seen, a continuous star formation burst must be considered, which is not the case for NGC 4449.

Using Balmer line intensities, Böker et al. (2001) estimated that the stellar population in the nucleus is about 6-10 Myr. From HST/WFPC2 and infrared spectra, Gelatt et al. (2001) obtained for the nucleus an age of 8-15 Myr, and for some stellar clusters an age between 10 Myr and 1 Gyr. An age of 6.4 Myr was estimated by Hill et al. (1998) for the H II region. All these studies are consistent with the FUV spectral synthesis. The metallicity of NGC 4449 was estimated to be $12+\log[\text{O}/\text{H}]=8.4$, i.e. $1/2 Z_{\odot}$, according to Heckman et al. (1998).

Adopting a single burst model for both the nucleus and the H II region, we find that the internal extinction is 0.01 ± 0.01 , using $E(B-V)_{Gal}=0.019$ (NED). The continuum is very blue and difficult to fit properly. This is consistent with the presence of an underlying older population contributing to the FUV spectra, in addition to a younger one. The corrected FUV fluxes then give stellar masses of $1.3\text{-}2.0\times 10^6 M_{\odot}$ for each of the nucleus and the H II region. Gelatt et al. (2001) and Böker et al. (2001) obtained stellar masses of 2 and $4\times 10^5 M_{\odot}$ for the nuclear region, which is a factor of two lower than the FUV result. However, Böker et al. (2001) used a $2''\times 2''$ aperture, significantly smaller than the LWRs/FUSE aperture, which can explain the difference. Hill et al. (1998) used a large $0.39'$ circular aperture to observe the H α flux in the H II region. Their result, 3.2×10^{-12} ergs s $^{-1}$ cm $^{-2}$ Å $^{-1}$ is very similar to the values predicted by a single population. Other predicted values are given in Table 4. It is rather difficult to compare them to published data because of large differences between apertures.

NGC 1140 is an irregular BCD containing numerous H II regions (Hodge & Kennicutt 1983). A fair quality spectrum ($S/N\approx 8$; see Fig. 6) has been obtained with FUSE. The line depth of C III and P v are better reproduced by a model at Z_{\odot} . The faint P Cygni absorption seen in the blue wing of C III is better reproduced with a population of 5.0 Myr, while the P v doublet favors a population of 6.0 Myr. A compromise for the two indicators is a 5.0 ± 1.0 Myr instantaneous burst. Note that an IMF slope of 2.8 improves the line fitting, especially for the P v feature. Continuous burst models cannot reproduce the diagnostic line profiles. The young age found with FUV data is consistent with those given in

the literature (Guseva, Izotov, & Thuan 2000; Bonatto et al. 1999). As for NGC 4449, the steep IMF slope found here is interpreted as an indication of multiple burst superposition, all with a standard IMF slope, where one burst is dominated by B stars. Heckman et al. (1998) evaluated an abundance of $12+\log[\text{O}/\text{H}]=8.0$, or $0.2 Z_{\odot}$, while it would be of 8.46, or $0.6 Z_{\odot}$, according to Guseva et al. (2000). The last value is in better agreement with the line depth seen in the FUV.

By comparing the observed FUV slope continuum to the best single burst model with $\alpha=2.8$, we find $E(B-V)_i=0.08\pm 0.08$ using $E(B-V)_{Gal}=0.038$ (NED). This extinction is in good agreement with the optical values of 0.10 and 0.18 obtained by Storchi-Bergmann et al. (1994) and Calzetti et al. (1995), respectively. Correcting for dust, we estimate a stellar mass of 5.6×10^6 to $1.6\times 10^8 M_{\odot}$. H α fluxes of 1.4 to 1.9×10^{-12} ergs s $^{-1}$ cm $^{-2}$ Å $^{-1}$, measured by several authors (Mazzarella & Boroson 1993; Calzetti et al. 1995; Storchi-Bergmann et al. 1995; Rosa-González, Terlevich & Terlevich 2002), are consistent with predictions reported in Table 4. A EW(H α) of 138.5 Å (Mazzarella & Boroson 1993) and a continuum level of 1.4×10^{-14} at 5500 Å (Storchi-Bergmann et al. 1995) also correspond relatively well to the FUV predictions taking into account the aperture sizes. Guseva et al. (2000) measured a much lower value for the H α flux. Based on the H β line and the WR bump at 4686 Å, they also estimated the presence of 15 547 O and 461 WNL stars, which are in agreement with the predictions within the given uncertainties.

4.5 Other Starbursts: FUSE spectra with a lower signal

NGC 4194 is classified as a BCD galaxy. The spectrum collected by FUSE for this target is rather noisy ($S/N\approx 6$; see Fig. 8), especially in the C III line section where only the LiF1B segment contributes. Furthermore, the P v $\lambda 1118$ line is contaminated by an airglow line. Despite these observational constraints, we obtain a reliable fit to the stellar lines using an instantaneous burst model of 5.5 ± 0.5 Myr with a solar metallicity. An IMF slope of 2.35 is simply adopted here because of the low S/N. A continuous burst models cannot reproduce the data.

Few studies have been published about the stellar populations of NGC 4194. Calzetti (1997) estimates its metallicity to $1.26 Z_{\odot}$ (i.e. $12+\log[\text{O}/\text{H}]=8.81$), consistent with the FUV line profiles. Kinney et al. (1993) have detected Si IV and C IV lines in IUE spectra, signatures of massive stars. Their flat UV continuum strongly suggests the presence of A-type stars. Based on the UV flat continuum, Bonatto et al. (1999) estimate an age of 10 to 25 Myr for the stellar population. From our FUV data, we are confident that a very young population of 5.5 ± 0.5 Myr is also present in NGC 4194. With a higher S/N, it would have been possible to better constrain the IMF slope and maybe see indications of an older population (see §4.4).

IRAS 19245-4140 (or Tol 1924-416) is a BCD galaxy. The observed FUV spectrum of IRAS 19245-4140 is presented in Figure 8, showing a S/N of 6. The best fit for the relatively shallow stellar line profiles is obtained for an instantaneous models at $0.4 Z_{\odot}$. An instantaneous burst with an age of 3.5 to 6.0 Myr is ideal to reproduce the observed C III line while an age of 4.5 to 6.0 Myr gives better results for

the P v doublet. We therefore adopt an age of 5.0 ± 1.0 Myr. A standard IMF was adopted because of the low S/N. A continuous burst scenario is never satisfying because the observed C III line does not display any P Cygni profile and the observed P v lines are too narrow. An age of 5 Myr is in agreement with other works (Bergvall 1985; Kinney et al. 1993; Raimann et al. 2000; Bonatto et al. 2000). Based on the flux measurements of nebular lines from Bergvall (1985), we calculate an oxygen abundance of $12 + \log[\text{O}/\text{H}] = 8.1$ ($0.25 Z_{\odot}$) for IRAS 19245+4140, consistent with FUV synthesis.

From the FUV continuum slope, we find an internal extinction of $E(B-V) = 0.1 \pm 0.1$, with a better fit if the extinction is closer to zero. This result agrees with the low reddening found by Storchi-Bergmann et al. (1994) and Calzetti et al. (1995). The observed FUV flux level leads to a stellar mass of $10^6 - 10^8 M_{\odot}$ for the young burst. The H α fluxes measured by Storchi-Bergmann et al. (1995) and Calzetti et al. (1995) are consistent with LavalSB calculations (Tab. 4). The F(5500) value obtained by Storchi-Bergmann et al. (1995) is also in agreement with the predictions. Raimann et al. (2000) also see an old population of ~ 100 Myr in addition to the young one. However the presence of the second component is impossible to establish from FUV data.

NGC 3504 is a spiral galaxy composed of a young nuclear starburst and a non-thermal source (Keel 1984). Figure 8 shows the FUSE spectrum of NGC 3504 with $S/N \simeq 8$. From the presence of stellar wind features, it is clear that the nuclear burst dominates the non-thermal source and can easily be studied at short wavelengths. Note the presence of an airglow line near P v $\lambda 1128$. The wind signatures are so pronounced that a model at $2 Z_{\odot}$ and a very young age of 2.5-3.5 Myr is required, with a better fit at 2.5 Myr. As shown in Figure 8, the observed stellar lines are not perfectly fitted by the best model due to the lack of an appropriate spectral library at high metallicity (see §3). Because of the limitation imposed by the spectral library, we simply adopted a standard IMF slope. Based on the line behavior of models at Z_{\odot} , continuous burst scenarios have been rejected because they cannot reproduce the strong P Cygni for the C III line. Other studies on NGC 3504 mostly focus on the non-thermal source, but the few ones treating the galaxy stellar populations seems to be in good agreement with FUV synthesis (Sekiguchi & Anderson 1987; Terlevich, Díaz & Terlevich 1990; Kinney et al. 1993; Elmegreen et al. 1997). The galaxy is metal rich, with $2.5 Z_{\odot}$ according to Heckman et al. (1998), which is consistent with the FUV synthesis.

Using a Galactic extinction of 0.027 (NED), we calculate that $E(B-V)_i = 0.30 \pm 0.05$, leading to $\text{Log}(M_*) = 8.8 \pm 0.5 M_{\odot}$. This mass is an upper limit since we did not consider a contribution from the non-thermal source. Other calculated parameters are given in Table 4. However, the lack of studies on the stellar content of NGC 3504 allows no more comparison.

NGC 5194 (M 51) is part of an interacting system with NGC 5195, and is known as the Whirlpool nebula. A faint non-thermal source has also been observed in the nucleus (Heckman, Crane & Balick 1980). Five data sets centered on various regions of NGC 5194 have been obtained with FUSE. Three of these sets have a poor quality while the

two other sets have S/N of ~ 3 (B10601 and B10604), which are also individually too low for synthesis. The B10601 set is centered on the nucleus and the B10604 targets a bright H II region located 2' North of the nucleus. Amazingly, although they include very different physical regions, these two spectra look similar with broad P Cygni profiles lost into the noise. Therefore, in order to increase the S/N and facilitate the synthesis, we decided to combine the two data sets. A careful interpretation is then recommended as if the final spectrum was obtained, roughly, through a larger aperture.

The combined FUV spectrum is shown in Figure 8. The resulting S/N is of ~ 4 , barely enough for the spectral synthesis. As for M 83 and NGC 3504 (Fig. 1 and 8, respectively), the broad wind profile in C III suggests a young and metal rich stellar population. Considering models at Z_{\odot} and $2 Z_{\odot}$, and adopting a standard IMF, we can reproduce the diagnostic lines with an instantaneous burst of 3.0-3.5 Myr. If we try to perform the synthesis on the individual sets of observation, we roughly obtained an age of about 2 and 4 Myr for the H II region and the nucleus, respectively. Therefore, the age obtained for the average spectrum seems meaningful taking into account the differences between the two regions, the low S/N, and the lack of a metal rich spectral library (see §3). The HUT spectrum of NGC 5194 studied by Leitherer et al. (2002a) revealed an age of ~ 5 Myr, in good agreement with the FUV synthesis. The IUE spectrum from (Kinney et al. 1993) suggests that the dominant stars in NGC 5194 are A- and G-type stars. In any case, such stars are too cold to be detected below 1200Å. Zaritsky et al. (1994) measured an oxygen abundance of 9.2, corresponding to $3.1 Z_{\odot}$, in the central region, consistent with the strong FUV wind profile of C III.

Using a model of 3.5 Myr at $2 Z_{\odot}$ and a Galactic extinction of 0.035 (NED), we measure an internal extinction of 0.25 ± 0.15 , which leads to a global stellar mass of the order of $10^7 M_{\odot}$. Predicted values obtained from the combined FUSE data sets are reported in Table 4. If these values are to be compared with observations, one must remember to consider the global flux from the nucleus and the H II region and also to take into account the non-thermal contribution.

NGC 3991 is a Magellanic type galaxy, member of the interacting system which includes NGC 3994 and NGC 3995 (Keel et al. 1985). It contains about 25 stellar clusters (Meurer et al. 1995), probably responsible for most of the FUV flux. Figure 8 shows the observed spectra obtained for NGC 3991 ($S/N \simeq 6$). Because of the redshift, the C III structure is incomplete. However, the presence of an extended absorption in the blue wing of C III, due to evolved O stars, is evident. Models at Z_{\odot} correspond well to the observed line strengths of P v. The best-fitting for the P v doublet is obtained at 4.0-4.5 Myr with $\alpha = 2.8$, especially to fit the P v $\lambda 1128$ P Cygni profile. An instantaneous burst of 3.5-4.0 Myr can reproduce the C III blue wing for both IMF slopes of 2.35 and 2.8. We then conclude that the young stellar population of NGC 3991 is dominated by massive stars of 4.0 ± 0.5 Myr at $\sim Z_{\odot}$ with an IMF slope of $\sim 2.35 - 2.8$. Although the noise level in the FUV spectrum of NGC 3991 is relatively high, the steep IMF slope suggests that one or several older bursts, dominated by B stars, may contribute to the FUV line profiles. As for NGC 7714, it is possible to reproduce the observed line profiles with a continuous burst of star formation, but we suspect that this is not real

as a result of a degeneracy effect between an instantaneous model at 4.5 Myr and a continuous burst of 10-20 Myr. According to the work of Bonatto et al. (1999), about 60% of the flux at 2646Å is produced by O-type stars of less than 5 Myr, consistent with the FUV synthesis for an instantaneous burst. Heckman et al. (1998) estimated the metallicity of NGC 3991 to $0.6 Z_{\odot}$, indicating that the FUV models at Z_{\odot} can fit a wide range toward lower metallicities.

Adopting the instantaneous burst scenario and a $E(B-V)_{Gal}=0.022$ (NED), we estimate the internal extinction value to 0.3 ± 0.1 . This value is higher than the 0.07 value obtained by Meurer et al. (1995). The $E(B-V)_i$ implies a stellar mass of 10^9 to $10^{11} M_{\odot}$. Unfortunately, the FUV synthetic results cannot be fully tested since very few works are related to the stellar populations of NGC 3991. The observed $H\alpha$ flux values, uncorrected for extinction, obtained by Dahari (1985), Keel et al. (1985), and Meurer et al. (1995) with various apertures are between 2 and 3×10^{-13} ergs $s^{-1} cm^{-2} \text{ \AA}^{-1}$, a factor of 10^3 lower than the LavalSB calculation.

NGC 7673 (Mrk 325) displays numerous aggregates (Benvenuti, Casini & Heidmann 1982). Figure 8 shows the observed FUV spectrum with S/N=9, which includes most of the known star clusters. The C III line is incomplete because of the galaxy redshift, but the C III blue wing do not show obvious absorption in comparison to NGC 3991 (having a similar redshift). This suggests an older burst and/or a lower metallicity. The C III and P v lines are indeed well reproduced by an instantaneous burst of 6.5 ± 0.5 Myr at Z_{\odot} with $\alpha(\text{IMF})=2.35-2.8$. Continuous models do not reproduce the observed P v line profiles. A steep IMF slope suggests the superposition of an older burst dominated by B stars (§4.4), which seems to be consistent with the IUE spectrum of Kinney et al. (1993) where an important contribution from B-type stars is observed. Bonatto et al. (1999) also concluded that 50% of the UV flux comes from OB stars. (Heckman et al. 1998) give a metallicity of $0.6 Z_{\odot}$ for NGC 7673, which is consistent with the range of metallicity covered by the Z_{\odot} model (see also NGC 1140 in §4.4).

Adopting a burst of 6.5 Myr at Z_{\odot} and a standard IMF, we estimate an internal extinction of 0.07 ± 0.07 , with a better fit closer to zero, using $E(B-V)_{Gal}=0.043$ (NED). This value is much below the $E(B-V)_i$ of 0.42 obtained by Storchi-Bergmann et al. (1994) from the Balmer decrement through a $10''\times 20''$. Although the Balmer decrement usually gives twice the extinction values based on stellar indicators, this is still high compared to the FUV result. However the low extinction gives a stellar mass of $\sim 10^7 M_{\odot}$ which is consistent to the $9\times 10^7 M_{\odot}$ estimated by Duflot-Augarde & Alloin (1982) through a $40''\times 40''$ aperture. The predicted $H\alpha$ and F(5500) fluxes (see Tab. 4) are in agreement with the observations of McQuade, Calzetti & Kinney (1995; circular aperture of $13.5''$). An $EW(H\alpha)$ of 106\AA measured by Keel & van Soest (1992) is in good agreement with the FUV predictions.

Mrk 054 is a very blue starburst galaxy (Gondhalekar et al. 1984; Kinney et al. 1993) and one of the most distant object of the sample ($z=0.045$). Because of the large redshift, the C III line is outside of the FUSE wavelength range (see Fig. 8). Furthermore, the P v $\lambda 1118$ line is contaminated by an airglow emission. Fortunately, the S/N ratio of the FUSE spectrum is good enough and

the P v lines can still be used for the synthesis. The P v line profiles suggest a metallicity around solar and an age of (10 ± 1) Myr. A standard IMF has been assumed. There is no work in the literature that can help us confirm the metallicity of Mrk 054. Bonatto et al. (2000) estimate that 54% of the flux at 2646Å from IUE data comes from a young stellar population of ~ 2.5 Myr.

With a 10 Myr burst at Z_{\odot} and a Galactic extinction of 0.015 (NED), we find an internal extinction of 0.1 ± 0.1 , with a better fit closer to zero. It corresponds to the estimation of Bonatto et al. (2000). This value leads to a stellar mass of $\sim 10^8 M_{\odot}$. Model predictions are listed in Table 4. Maehara et al. (1987) obtained $EW(H\alpha)=40\text{\AA}$, which is quite high compared to the LavalSB calculation of $11\pm 6\text{\AA}$, but the uncertainty on the result of these authors may be large as they used photographic plates.

Tol 0440–381 is the second most distant object of our sample ($z=0.041$). Because of the redshift, the C III line is not observed (see Fig. 8). The P v $\lambda 1118$ line is dominated by noise. Synthesis is then restricted to the P v $\lambda 1128$ line. Models at Z_{\odot} are good to reproduce the line depth, but the absence of the C III feature combined with the noise does not allow to really distinguish between the solar and sub-solar metallicities. The best fit is obtained for an instantaneous burst of 5.0 Myr, while ages between 4.5 to 6.0 Myr are suitable. A standard IMF has been assumed. A few studies on Tol 0440–381 focus on stellar populations (Masegosa, Moles & del Olmo 1991; Raimann et al. 2000). They are usually very consistent with the FUV synthesis since they report the presence of WR signatures. From nebular line intensities obtained by Terlevich et al. (1991), we calculated an oxygen abundance of 8.2 ($0.3 Z_{\odot}$), in agreement with Denicoló et al. (2002). This favors sub-solar metallicity models for the FUV synthesis.

Using $E(B-V)_{Gal}=0.015$ (NED), we obtain that $E(B-V)_i=0.20\pm 0.15$, similar to the nebular value of 0.24 obtained by Cerviño & Mas-Hesse (1994). This extinction gives a stellar mass around $10^9 M_{\odot}$ for the burst. **As for IRAS 08339+6517, the stellar mass value of Tol 0440–381 shows large uncertainties due to a shorter wavelength coverage and large uncertainties on the extinction value. This mass value must be interpreted with care.** The optical values predicted from the FUV information are in relative good agreement with the observations of Campbell, Terlevich & Melnick (1986) and Terlevich et al. (1991) considering the differences in aperture size and uncertainties.

4.6 Young Stellar Populations in Seyfert Galaxies

NGC 1672 shows a Seyfert 2 type nuclear activity (Mouri et al. 1989) as well as a nuclear ring of intense star formation (e.g. Storchi-Bergmann, Wilson & Baldwin 1996). The FUSE spectrum of NGC 1672, centered on the nucleus (Fig. 9), displays a broad and deep C III line profile, suggesting the presence of evolved metal rich O-type stars. The P v $\lambda 1118$ line is contaminated by an important airglow emission. Models at $2 Z_{\odot}$ are required to explain the line width and depth of C III, and a better fit is obtained for a 3.5 ± 1.0 Myr population. P v lines can be reproduced by a model at 3.5-4.0 Myr. Overall, the best fit is obtained for a 3.5 ± 1.0 Myr instantaneous burst. A stan-

standard IMF slope has been assumed because of the spectral library limitation at this metallicity. Bonatto et al. (1998) calculated that the dominating stellar population at 2646Å is 10^8 yr (but these older stars do not emit below 1200Å) and that stars of less than 20 Myr contribute to less than 20% to the flux. García-Vargas et al. (1990) synthesized the IUE spectrum of NGC 1672 and obtained an age of about 8 Myr for the burst, still older than what is suggested by the strong P Cygni profile in C III. In agreement with the FUV synthesis, Zaritsky et al. (1994) measured an abundance $12+\log[\text{O}/\text{H}]=9.1$ ($\sim 2.5 Z_{\odot}$) and supported by Storchi-Bergmann et al. (1996, 1998) who found a similar value of 9.2.

Considering a Galactic extinction of 0.023 (NED), we find an internal extinction of 0.15 ± 0.10 . This is relatively consistent with the extinction of 0.6 obtained by Storchi-Bergmann et al. (1994) with the Balmer decrement, considering the uncertainties. The mass of the young stellar population estimated from the FUV flux is about $10^7 M_{\odot}$, which is an upper limit considering the non-thermal source. However, according to Heckman et al. (1995), a maximum of 20% of the flux at 1500Å in Seyfert 2 nuclei comes from the non-thermal source. This contribution seems to be generally lower than 10% (Heckman et al. 1997; González Delgado et al. 1998b). The optical flux values reported in Table 4 are higher than the observations of Storchi-Bergmann et al. (1995). This can be explained by the presence of the non-stellar activity. Underlying stellar populations could also contribute to the optical flux.

NGC 7496 is a barred spiral galaxy with a Seyfert 2 nucleus. The nuclear region also displays many H II regions (Véron et al. 1981), which are responsible for an intense far-infrared luminosity. The FUSE spectrum shows strong evidence for such OB stars (Fig. 9) with a well-developed wind profile in C III. An airglow line is superposed to the P v $\lambda 1128$ line. The comparison with FUV synthetic spectra suggests a metallicity higher than solar, and an age of 2.5 ± 0.5 Myr, assuming a standard IMF. This age is consistent with the result of Bonatto et al. (1998). The metallicity of the nucleus is known to be around $2 Z_{\odot}$ ($12+\log[\text{O}/\text{H}]=9.0$; Heckman et al. 1998), also in agreement with the FUV synthesis.

Comparing the observed and synthetic FUV continuum slopes, we obtain that $E(B-V)_i=0.03\pm 0.02$, with a better fit closer to zero, and using a Galactic extinction of 0.01 (NED). This extinction is much lower than the 0.6 value obtained by Storchi-Bergmann et al. (1994). The FUV flux implies a stellar mass of $3\text{-}10\times 10^5 M_{\odot}$, which is an upper limit considering that the non-thermal source is also contributing to the FUV flux. Storchi-Bergmann et al. (1995) measured $F(\text{H}\alpha)=5.8\times 10^{-13}$ ergs s^{-1} cm^{-2} \AA^{-1} consistent with the prediction, but they also obtained $F(5500)=9.9\times 10^{-15}$ ergs s^{-1} cm^{-2} \AA^{-1} , which is slightly higher than the predictions reported in Table 4. The difference can be explained by the non-thermal activity and/or underlying older stellar populations.

NGC 1667 is a Seyfert 2 galaxy where several H II regions are observed along the spiral arms and in a nuclear ring (González Delgado et al. 1997b). Thuan (1984) studied the IUE spectrum of NGC 1667 and concluded that the active nucleus is lying in an important starburst. As shown in Figure 9, although the C III line is missing because of

the redshift, stellar lines of P v are clearly observed. The O VI doublet (not shown) also displays a P Cygni profile, which confirms the young stellar population contribution in the FUV range. The P v line depth suggests a metal rich population at Z_{\odot} or $2 Z_{\odot}$, but it is impossible to distinguish between the two metallicities without the C III line. Adopting a standard IMF, an age of 5.0 ± 0.5 Myr is obtained if the metallicity is Z_{\odot} , or 4.0 ± 1.0 Myr if we use a $2 Z_{\odot}$ model. These ages are consistent with previous works (Thuan 1984; Bonatto et al. 1998). Storchi-Bergmann, Bica & Pastoriza (1990) measured the nitrogen and sulfur abundances of NGC 1667 and, taking into account the contamination by the active nucleus, they obtained a high metallicity around $3 Z_{\odot}$.

Considering the observed metallicity, we adopt the model at 4.0 Myr and $2 Z_{\odot}$ for NGC 1667, and we find an internal extinction of 0.08 ± 0.08 using a $E(B-V)_{Gal}=0.0$. We calculated that $\text{Log}(M_{\star})=7.5_{-1}^{+0.5}$, which is only an upper limit since the AGN also contribute to the flux measured by FUSE. Predicted fluxes in the visible range (Tab. 4) are also higher limits. The predicted values are in agreement with the observations (McQuade et al. 1995; Storchi-Bergmann et al. 1995; Ho, Filippenko & Sargent 1997; Thuan 1984), considering the uncertainties.

NGC 1068 (M 77) is a nearby spiral galaxy ($z=0.0038$) well-studied for its Seyfert 2 nucleus and its nuclear ring of star formation (e.g. Antonucci & Miller 1985). The FUSE spectrum of the central $30''\times 30''$ is presented in Figure 9. It displays broad and extremely shallow absorption features at wavelengths corresponding to the stellar lines. However, no model for a young stellar population can reproduce these unusual profiles. In Figure 9, the synthetic spectrum for an instantaneous burst of 5 Myr at Z_{\odot} with a standard IMF slope is shown superposed to the observation for a simple comparison. It seems here that very massive stars may contribute to the spectrum, but they are strongly diluted by an additional continuum, likely from the active nucleus. However, our attempt to include a featureless power-law continuum to the synthetic spectrum of a stellar population was not successful.

4.7 Seyfert Galaxies Dominated by Non-Stellar Activity

NGC 4151 is classified as a Seyfert 1.5 galaxy because of its remarkable flux variabilities between the Seyfert 1 and 2 types. During its low activity phase, absorption features are observed in the FUV (Fig. 9). A closer look at these lines reveals that they are blueshifted by 2-3Å compared to the synthetic stellar features of a 10 Myr burst at Z_{\odot} . The FUSE spectrum was corrected for the radial velocity of 995 km s^{-1} as given by NED. We also noted that the O VI feature do show non-stellar features in emission. Despite the fact that the observed line profiles in NGC 4151 may mimic the usual diagnostic lines of young starbursts, we are actually looking at signatures from hot gas located very near the central engine, ionized, and pushed away from it as shown by e.g. Kriss et al. (1992), Espey et al. (1998), and Crenshaw et al. (1999). This explain the shifted features and consequently no signature of massive stars are detected within the FUSE aperture.

NGC 3783, NGC 7469, and NGC 5548 are

Seyfert 1 galaxies for which FUSE obtained a spectrum with a good S/N (see the example of NGC 3783 in Fig. 9). As expected, the FUV spectrum of these three Seyfert 1 nuclei are entirely dominated by the non-thermal activity and no obvious absorption features, other than interstellar lines or detector defects, was observed. At shorter wavelengths, the FUSE spectra of these objects (see e.g. Kriss et al. 2003) display a flat continuum with broad emission lines for e.g. C III λ 977, N III λ 991, the O VI $\lambda\lambda$ 1032, 1038 doublet, and the He II λ 1085 line. These objects are dominated by the non-thermal source and, if present, signature of massive stars are completely diluted.

5 CONCLUSION

In this work, we characterized the physical properties of very young stellar populations contained in 24 local starbursts. FUSE data and evolutionary spectral synthesis with `Lava1SB` allowed us to obtain accurate ages, estimates of stellar masses and internal extinctions. We also calculated and compared values for several parameters in the visible range produced by the young stellar populations observed in the FUV.

While the metallicity cannot be evaluated with a great precision, we were able to distinguish between 4 metallicity ranges corresponding to the 4 evolutionary track metallicities used by `Lava1SB`. Unlike the UV wavelength range above 1200Å, we were able to distinguish between solar metallicity and richer populations due to unsaturated C III line profile. In a few cases where the FUV synthesis indicated a solar metallicity (NGC 1140, NGC 4449, NGC 7673), we found that the literature was sometimes proposing a lower value, but still higher than the LMC metallicity. We therefore conclude that the FUV line profiles may be less sensitive to the metallicity between values of $\sim Z_{\odot}$ and $0.4 Z_{\odot}$. Although our low metallicity models are limited by the lack of B-type stars, we were able to clearly identify low metallicity stellar populations and to estimate a lower age limit (i.e. NGC 1705, I Zw 18).

From the FUV point of view, star formation in starbursts seems to occur on a very short period of time, favoring the instantaneous burst scenario. In most cases, continuous star formation models obviously did not represent the observed situations. The predominance of instantaneous bursts in our sample of starburst galaxies is likely the result of an observational bias. The bias is due to the continuum flux level of individual O and B stars below 1200Å, which varies significantly from one spectral type to another. The effect is present above 1200Å, but is more dramatic below 1200Å because the SED of OB stars in the FUV is coincident with the peak of their black body radiation spectrum. A small variation of temperature will affect significantly more the bluer side of the black body radiation spectrum than the redder side. Consequently, any property derived from stellar line profiles in the FUV range is biased toward the young populations. This idea is supported by the work of Bruhweiler, Miskey, & Smith Neubig (2003) where they compared the UV line profiles of individual massive stars observed in NGC604 with those of the integrated spectrum. They found that a very small number (10) of very bright stars dominate the line profiles of the whole stellar cluster.

When looking at starburst galaxies in the FUV with a large aperture, it should not be surprising to see that young populations of a few Myr preferably show up and that the stellar line profiles are in better agreement with instantaneous burst models.

For spectra having a sufficient S/N, we constrained the IMF slope using the sensitivity of line profiles. In general, the IMF slope α is near 2.35. We used this property to detect underlying stellar populations dominated by B-type stars in NGC 4449, NGC 3991, and NGC 1140, probably resulting from one or several previous burst event a few 10^7 to 10^8 years ago.

We also detected very young stellar populations of less than 5 Myr in Seyfert 2 nuclei. However, no sign of such population has been detected in Seyfert 1 nuclei, the central engine being dominant in flux.

ACKNOWLEDGMENTS

The authors thanks C. Leitherer for comments on the manuscript. This work was supported by the Natural Sciences and Engineering Research Council of Canada and by the Fonds FCAR of the Government of Québec. This research has made use of the NASA/IPAC Extragalactic Database (NED) which is operated by the Jet Propulsion Laboratory, California Institute of Technology, under contract with the NASA.

REFERENCES

- Aloisi, A., Tosi, M., Greggio, L., 1999, *AJ*, 118, 302
- Aloisi, A., Savaglio, S., Heckman, T. M., Hoopes, C. G., Leitherer, C., Sembach, K. R. 2003, *ApJ*, 595, 760
- Alonso-Herrero, A., Rieke, G. H., Rieke, M. J., Scoville, N. Z., 2000, *ApJ*, 532, 845
- Annibali, F., Greggio, L., Tosi, M., Aloisi, A., Leitherer, C. 2003, *AJ*, 126, 2752
- Antonucci R. & Miller J. S., 1985, *ApJ*, 297, 621
- Benvenuti, P., Casini, C., Heidmann, J., 1982, *MNRAS*, 198, 825
- Bergvall, N., 1985, *A&A*, 146, 269
- Boisson, C., Joly, M., Moulataka, J., Pelat, D., Serote Roos, M., 2000, *A&A*, 357, 850
- Böker, T., van der Marel, R. P., Mazzuca, L., Rix, H.-W., Rudnick, G., Ho, L. C., Shields, J. C., 2001, *AJ*, 121, 1473
- Bonatto, C., Pastoriza, M. G., Alloin, D., Bica, E., 1998, *A&A*, 334, 439
- Bonatto, C., Bica, E., Pastoriza, M. G., Alloin, D., 1999, *A&A*, 343, 100
- Bonatto, C., Bica, E., Pastoriza, M. G., Alloin, D., 2000, *A&A*, 355, 99
- Bresolin, F. Kennicutt, R. C., 2002, *ApJ*, 572, 838
- Bruhweiler, F. C., Miskey, C. L., Smith Neubig, M. 2003, *AJ*, 125, 3082
- Bruzual, G., Charlot, S., 2003, *MNRAS*, 344, 1000
- Buat, V., Burgarella, D., Deharveng, J. M., Kunth, D., 2002, *A&A*, 393, 33
- Calzetti, D., Bohlin, R. C., Kinney, A. L., Storchi-Bergmann, T., Heckman, T. M., 1995, *ApJ*, 443, 136

- Calzetti, D., Meurer, G. R., Bohlin, R. C., Garnett, D. R., Kinney, A. L., Leitherer, C., Storch-Bergmann, T. 1997, *AJ*, 114, 1834
- Calzetti, D., 1997, *AJ*, 113, 162
- Calzetti, D., Conselice, C. J., Gallagher, J. S., Kinney, A. L., 1999, *AJ*, 118, 797
- Campbell, A., Terlevich, R., Melnick, J., 1986, *MNRAS*, 223, 811
- Cannon, J. M., Skillman, E. D., Kunth, D., Leitherer, C., Mas-Hesse, M., Ostlin, G., Petrosian, A. 2004, *ApJ*, 608, 768
- Cannon, J. M., Skillman, E. D., Garnett, D. R., Dufour, R. J., 2002, *ApJ*, 565, 931
- Cardelli, J. A., Clayton, G. C., Mathis, J. S., 1989, *ApJ*, 45, 245
- Cerviño, M. & Mas-Hesse, J. M., 1994, *A&A*, 284, 749
- Chandar, R., Leitherer, C., Tremonti, C. A., 2004, *ApJ*, 604, 153
- Charbonnel, C., Meynet, G., Maeder, A., Schaller, G., Schaerer, D., 1993, *A&AS*, 101, 415
- Crenshaw, D. M., Kraemer, S. B., Boggess, A., Maran, S. P., Mushotzky, R. F., Wu, C.-C., 1999, *ApJ*, 516, 750
- Crowther, P. A., Hillier, D. J., Evans, C. J., Fullerton, A. W., De Marco, O., Willis, A. J. 2002, *ApJ*, 579, 774
- Crowther, P. A., Hadfield, L. J., Schild, H., Schmutz, W. 2004, *A&A*, 419, L17
- Dahari, O., 1985, *ApJS*, 57, 643
- Denicoló, G., Terlevich, R., Terlevich, E., 2002, *MNRAS*, 330, 69
- Dionne, D. 1999, in van der Hucht, K.A., Koenigsberger, G., Eenens, P.R.J., eds, *Proc. IAU Symp. 193, Wolf-Rayet Phenomena in Massive Stars and Starburst Galaxies. Astron.Soc.Pac.*, San Francisco, p.596
- Dionne, D., Robert, C. 2006, *ApJ*, 641, 252
- Duflot-Augarde, R., Alloin, D., 1982, *A&A*, 112, 257
- Dufour, R. J., Garnett, D. R., Shields, G. A., 1988, *ApJ*, 332, 752
- Elmegreen, D. M., Chromey, F. R., Santos, M., Marshall, D., 1997, *AJ*, 114, 1850
- Elmegreen, D. M., Chromey, F. R., Warren, A. R., 1998, *AJ*, 116, 2834
- Elmegreen, D. M., Chromey, F. R., McGrath, E. J., Ostenson, J. M., 2002, *AJ*, 123, 1381
- Espey, B. R., Kriss, G. A., Krolik, J. H., Zheng, W., Tsvetanov, Z., Davidsen, A. F., 1998, *ApJ*, 500, L13
- Fernandes, I. F., de Carvalho, R., Contini, T., Gal, R.R., 2004, *MNRAS*, 355, 728
- Friedman, S. D., Cohen, R. D., Jones, B., Smith, H. E., Stein, W.A., 1987, *AJ*, 94, 1480
- García-Vargas, M. L., Díaz, A. I., Terlevich, R. J., Terlevich, E., 1990, *AP&SS*, 171, 65
- García-Vargas, M. L., González-Delgado, R. M., Perez, E., Alloin, D., Díaz, A., Terlevich, E., 1997, *ApJ*, 478, 112
- Gehrz, R. D., Sramek, R. A., Weedman, D. W., 1983, *ApJ*, 267, 551
- Gelatt, A. E., Hunter, D. A., Gallagher, J. S., 2001, *PASP*, 113, 142
- Gondhalekar, P. M., Morgan, D. H., Dopita, M., Phillips, A. P., 1984, *MNRAS*, 209, 59
- González-Delgado, R. M., Perez, E., Díaz, A. I., García-Vargas, M. L., Terlevich, E., Vilchez, J. M., 1995, *ApJ*, 439, 604
- González Delgado, R. M., Leitherer, C., Heckman, T. M., 1997a, *ApJ*, 489, 601
- González Delgado, R. M., Perez, E., Tadhunter, C., Vilchez, J. M., Rodríguez-Espinosa, J. M., 1997b, *ApJS*, 108, 155
- González Delgado, R. M., Leitherer, C., Heckman, T. M., Lowenthal, J. D., Ferguson, H. C., Robert, C., 1998a, *ApJ*, 495, 698
- González Delgado, R. M., Heckman, T. M., Leitherer, C., Meurer, G., Krolik, J., Wilson, A. S., Kinney, A., Koratkar, A., 1998b, *ApJ*, 505, 174
- González Delgado, R. M., García-Vargas, M. L., Goldader, J., Leitherer, C., Pasquali, A., 1999, *ApJ*, 513, 707
- González Delgado, R. M., Heckman, T. M., Leitherer, C., 2001, *ApJ*, 546, 845
- Guseva, N. G., Izotov, Y. I., Thuan, T. X., 2000, *ApJ*, 531, 776
- Harris, J., Calzetti, D., Gallagher, J. S., Conselice, C. J., Smith, D. A., 2001, *AJ*, 122, 3046
- Heckman, T. M., Crane, P. C., Balick, B. 1980, *A&AS*, 40, 295
- Heckman, T. M., et al., 1995, *ApJ*, 452, 549
- Heckman, T. M., González Delgado, R., Leitherer, C., Meurer, G. R., Krolik, J., Wilson, A. S., Koratkar, A., Kinney, A., 1997, *ApJ*, 482, 114
- Heckman, T. M., Leitherer, C., 1997, *AJ*, 114, 69
- Heckman T. M., Robert, C., Leitherer, C., Garnett, D. R., van der Rydt, F., 1998, *ApJ*, 503, 646
- Hibbard, J. E., Yun, M. S., 1999, *AJ*, 118, 162
- Hill, R. S., Fanelli, M. N., Smith, D. A., Bohlin, R. C., Neff, S. G., O'Connell, R. W., Roberts, M. S., Smith, A. M., Stecher, T. P. 1998, *ApJ*, 507, 179
- Ho, L. C., Filippenko, A. V., Sargent, W. L. W., 1997, *ApJS*, 112, 315
- Hodge, P. W., Kennicutt, R. C., 1983, *AJ*, 88, 296
- Hughes, M. A. et al. 2005, *AJ*, 130, 73
- Hunter, D. A., Thronson, H. A., Jr., 1995, *ApJ*, 452, 238
- Izotov, Y. I., Foltz, C. B., Green, R. F., Guseva, N. G., Thuan, T. X., 1997, *ApJ*, 487, L37
- Izotov, Y. I., Chaffee, F. H., Foltz, C. B., Green, R. F.; Guseva, N. G., Thuan, T. X. 1999, *ApJ*, 527, 757
- Keel, W. C. 1984, *ApJ*, 282, 75
- Keel, W. C., Kennicutt, R. C., Hummel, E., van der Hulst, J. M., 1985, *AJ*, 90, 708
- Keel, W. C., van Soest, E. T. M., 1992, *A&AS*, 94, 553
- Kennicutt, R. C., 1992, *ApJ*, 388, 310
- Kinney, A. L., Bohlin, R. C., Calzetti, D., Panagia, N., Wyse, R. F. G., 1993, *ApJS*, 86, 5
- Kobulnicky, H. A., Skillman, E. D., 1996, *ApJ*, 471, 211
- Kriss, G. A. et al., 1992, *ApJ*, 392, 485
- Kriss, G. A., Blustin, A., Branduardi-Raymont, G., Green, R. F., Hutchings, J., Kaiser, M. E. 2003, *A&A*, 403, 473
- Kroupa, P., 2004, *NewAR*, 48, 47
- Kunth, D., Joubert, M. 1985, *A&A*, 142, 411
- Kunth, D., Matteucci, F., & Marconi, G., 1995, *A&A*, 297, 634
- Kunth, D., Östlin, G., 2000, *A&A Rev*, 10, 1
- Kurucz, R. L., 1992, in Barbury, B., Renzini, A., eds., *Proc. IAU Symp. 149, The Stellar Populations of Galaxies. Kluwer Academic Publ.*, Dordrecht, p.225
- Leitherer, C., Heckman, T. M., 1995, *ApJS*, 96, 9
- Leitherer, C., Vacca, W. D., Conti, P. S., Filippenko, A.

- V., Robert, C., Sargent, W. L. W., 1996, *ApJ*, 465, 717
- Leitherer, C. et al., 1999, *ApJS*, 123, 3
- Leitherer, C., Li, I.-H., Calzetti, D., Heckman, T. M., 2002, *ApJS*, 140, 303
- Leitherer, C., Calzetti, D., Martins, L. P., 2002, *ApJ*, 574, 114
- MacKenty, J. W., Maíz-Apellániz, J., Pickens, C. E., Norman, C. A., Walborn, N. R., 2000, *AJ*, 120, 3007
- Maehara, H., Noguchi, T., Takase, B., Handa, T., 1987, *PASJ*, 39, 393
- Margon, B., Anderson, S. F., Mateo, M., Fich, M., Massey, P., 1988, *ApJ*, 334, 597
- Mas-Hesse, J. M., Kunth, D., 1999, *A&A*, 349, 765
- Massey, P., 1998, in Gilmore, G. Howell, D., eds., *Proc. ASP Conf. Ser. Vol. 142, The Stellar Initial Mass Function*. Astron. Soc. Pac., San Francisco, p.17
- Masegosa, J., Moles, M., del Olmo, A., 1991, *A&A*, 244, 273
- Mazzarella, J. M., Boroson, T. A., 1993, *ApJS*, 85, 27
- McQuade, K., Calzetti, D., Kinney, A. L., 1995, *ApJS*, 97, 331
- Meurer, G. R., Heckman, T. M., Leitherer, C., Kinney, A., Robert, C., Garnett, D. R., 1995, *AJ*, 110, 2665
- Meynet, G., Maeder, A., Schaller, G., Schaerer, D., Charbonnel, C., 1994, *A&AS*, 103, 97
- Mollá, M., García-Vargas, M. L., 2000, *A&A*, 359, 18
- Moos, H. W., et al., 2000, *ApJ*, 538, L1
- Mouri, H., Taniguchi, Y., Kawara, K., Nishida, M., 1989, *ApJ*, 346, L73
- Östlin, G., 2000, *ApJ*, 535, L99
- Pagel, B. E. J., Simonson, E. A., Terlevich R. J., Edmunds, M. G., 1992, *MNRAS*, 255, 325
- Pastoriza, M. G., Dottori, H. A., Terlevich, E., Terlevich, R., Diaz, A. I., 1993, *MNRAS*, 260, 177
- Pellerin, A., 1999, MSc Thesis, Université Laval
- Pellerin, A., Fullerton, A. W., Robert, C., Howk, J. C., Hutchings, J. B., Walborn, N. R., Bianchi, L., Crowther, P. A., Sonneborn, G. 2002, *ApJS*, 143, 159
- Pellerin, A. 2004, PhD thesis, Université Laval.
- Puxley, P. J., Doyon, R., Ward, M. J., 1997, *ApJ*, 476, 120
- Raimann, D., Bica, E., Storchi-Bergmann, T., Melnick, J., Schmitt, H., 2000, *MNRAS*, 314, 295
- Robert, C. 1999, in Hubeny I., Heap S., Cornett R., eds, *ASP Conf. Ser. Vol. 192, Spectrophotometric Dating of Stars and Galaxies*. Astron. Soc. Pac., San Francisco, p. 16
- Robert, C., Pellerin, A., Aloisi, A. Leitherer, C., Hoopes, C. G., Heckman, T. M., 2003, *ApJS*, 144, 21
- Robert, C., Leitherer, C., Heckman, T. M., 1993, *ApJ*, 418, 749
- Rosa-González, D., Terlevich, E., Terlevich, R., 2002, *MNRAS*, 332, 283
- Sahnow, D. J., et al., 2000, *ApJ*, 538, L7
- Sargent, W. L. W., Filippenko, A. V., 1991, *AJ*, 102, 107
- Satyapal, S., Watson, D. M., Pipher, J. L., Forrest, W. J., Fischer, J., Greenhouse, M. A., Smith, H. A., Woodward, C. E., 1999, *ApJ*, 516, 704
- Sekiguchi, K., Anderson, K. S., 1987, *AJ*, 94, 644
- Schaller, G., Schaerer, D., Meynet, G., Maeder, A., 1992, *A&AS*, 96, 269
- Schaerer, D., Meynet, G., Schaller, G., 1993a, *A&AS*, 98, 523
- Schaerer, D., Charbonnel, C., Meynet, G., Maeder, A., Schaller, G. 1993b, *A&AS*, 102, 339
- Schaerer, D., Contini, T., Kunth, D., Meynet, G., 1997, *ApJ*, 481, L75
- Schaerer, D., Contini, T., Pindao, M., 1999, *A&AS*, 136, 35
- Schmidt-Kaler, T., 1982, in Schaifers, K., Voigt, H.H., eds., *Landolt-Börnstein IV: Numerical Data and Functional Relations in Science and Technology*. Springer-Verlag, Berlin, p.1
- Schmutz, W., Leitherer, C. Gruenwald, R. (1992), *PASP*, 104, 1164
- Smith, D. A. et al., 1996, *ApJ*, 473, L21
- Storchi-Bergmann, T., Bica, E., Pastoriza, M. G., 1990, *MNRAS*, 245, 749
- Storchi-Bergmann, T., Calzetti, D., Kinney, A. L., 1994, *ApJ*, 429, 572
- Storchi-Bergmann, T., Kinney, A. L., Challis, P., 1995, *ApJS*, 98, 103
- Storchi-Bergmann, T., Wilson, A. S., Baldwin, J. A., 1996, *ApJ*, 460, 252
- Storchi-Bergmann, T., Schmitt, H. R., Calzetti, D., Kinney, A. L., 1998, *AJ*, 115, 909
- Terlevich, E., Díaz, A. I., Terlevich, R., 1990, *MNRAS*, 242, 271
- Terlevich, R., Melnick, J., Masegosa, J., Moles, M., Copetti, M. V. F., 1991, *PASJ*, 91, 285
- Tinsley, B. M., 1968, *ApJ*, 151, 547
- Thuan, T. X., 1983, *ApJ*, 268, 667
- Thuan, T. X., 1984, *ApJ*, 281, 126
- Tosi, M., Sabbi, E., Bellazzini, M., Aloisi, A., Greggio, L., Leitherer, C., Montegriffo, P., 2001, *AJ*, 122, 1271
- Tremonti, C. A., Calzetti, D., Leitherer, C., Heckman, T. M., 2001, *ApJ*, 555, 322
- Vazdekis, A., 1999, *ApJ*, 513, 224
- Vázquez, G. A., Leitherer, C., Heckman, T. M., Lennon, D. J., de Mello, D. F., Meurer, G. R., Martin, C. L. 2004, *ApJ*, 600, 162
- Véron, P., Véron, M. P., Bergeron, J., Zuidervijk, E. J., 1981, *A&A*, 97, 71
- Walborn, N. R., Fullerton, A. W., Crowther, P. A., Bianchi, L., Hutchings, J. B., Pellerin, A., Sonneborn, G., Willis, A.J. 2002, *ApJ*, 141, 443
- Weedman, D. W., Feldman, F. R., Balzano, V. A., Ramsey, L. W., Sramek, R. A., Wu, C.-C., 1981, *ApJ*, 248, 105
- Willis, A. J., Crowther, P. A.; Fullerton, A. W., Hutchings, J. B., Sonneborn, G., Brownsberger, K., Massa, D. L., Walborn, N.R. 2004, *ApJS*, 154, 651
- Witt, A. N., Gordon, K. D., 2000, *ApJ*, 528, 799
- Worthey, G., Faber, S. M, González, J. J., Burstein, D., 1994, *ApJS*, 94, 687
- Zaritsky, D., Kennicutt, R. C., Huchra, J. P., 1994, *ApJ*, 420, 87

Table 1. Sample of Galaxies Observed with FUSE

Name	Morph/Activity	RA(J2000) (<i>h m s</i>)	DEC(J2000) (<i>° ' "</i>)	$E(B-V)_{Gal}^a$	D^b [Mpc]	FUSE ID	Exp. [sec]
IRAS 08339+6517	SB/starburst	08:38:23.20	+65:07:16.0	0.092	78.0	B00401	35162
IRAS 19245-4140	pec/Starburst	19:27:58.02	-41:34:27.7	0.00 ^c	36.5	A02306	4767
IZw 18	BCD	09:34:02.30	+55:14:25.0	0.00 ^c	14.3	P19801	31647
M 83	SAB(s)c/Starburst	13:37:00.51	-29:52:00.5	0.066	3.8	A04605	26528
MRK 054	Sc/Starburst	12:56:55.90	+32:26:52.0	0.015	180.0	A05201	25177
MRK 153	Sc/Starburst	10:49:05.15	+52:20:05.1	0.00 ^c	37.1	A09401	103724
NGC 1068	SA(rs)b/Syft 1-2	02:42:40.50	-00:00:51.7	0.034		A13902	75987
		02:42:40.72	-00:00:48.5			P11102	22579
NGC 1140	IBm pec/Syft 2	02:54:33.58	-10:01:39.9	0.038	19.6	A02305	4017
NGC 1667	SAB(r)c/Syft 2	04:48:37.14	-06:19:11.9	0.00 ^c	60.0	C04901	27651
NGC 1672	SB(r)bc/Syft 2	04:45:42.68	-59:14:49.7	0.023	15.5	C10901	11883
NGC 1705	SA0 pec/Starburst	04:54:13.48	-53:21:39.4	0.008	5.7	A04601	24026
NGC 3310	SAB(r)bc/Starburst	10:38:45.69	+53:30:06.0	0.022	17.9	A04602	26952
NGC 3504	SAB(s)ab/Starburst	11:03:11.21	+27:58:21.0	0.027	25.4	A02301	13455
NGC 3690	SB pec/H II	11:28:31.00	+58:33:41.0	0.017	45.0	B00402	59030
NGC 3991	Sm/Starburst	11:57:30.80	+32:20:12.1	0.022	46.3	A02302	6842
NGC 4151	SAB(rs)ab/Syft 1.5	12:10:32.58	+39:24:20.6	0.028		C09201	12916
		12:10:32.51	+39:24:20.8			P11105	20638
		12:10:32.60	+39:24:21.0			P2110201	14525
						P2110202	6601
NGC 4194	IBm pec/H II	12:14:09.70	+54:31:38.0	0.015	38.2	C04803	87236
NGC 4214	IAB(s)m/Starburst	12:15:39.41	+36:19:35.1	0.022	3.4	A04603	17981
NGC 4449-Nuc	IBm/Starburst	12:28:10.81	+44:05:42.9	0.00 ^c	3.1	A04606	8366
NGC 4449-HII	IBm/H II	12:28:09.37	+44:05:15.8		3.1	A04607	14042
NGC 5194	SA(s)bc pec/H II	13:29:52.35	+47:11:43.8	0.035	7.7	B10601	4473
		13:29:59.17	+47:13:53.9		7.7	B10604	3600
NGC 5253	Im pec/Starburst	13:39:55.97	-31:38:27.0	0.017 ^c	4.1	A04604	27344
NGC 7496	SB(rs)bc/Syft 2	23:09:47.27	-43:25:40.0	0.010	20.5	P10741	13305
NGC 7673	SAc pec/Starburst	23:27:41.59	+23:35:30.7	0.00 ^c	47.3	A02303	9930
NGC 7714	SB(s)b pec/Starburst	23:36:14.10	+02:09:18.6	0.08 ^d	37.5	A02304	8678
		23:36:14.00	+02:09:19.0		37.5	A08606	5970
		23:36:14.10	+02:09:19.0		37.5	B00403	16130
TOL 0440-381	BCD/WR+H II	04:42:08.03	-38:01:10.8	0.015	164.0	A05202	34411

^a From NED if nothing else is specified.

^b Distances from Heckman et al. (1998) and other authors cited in the text.

^c See text.

^d González Delgado et al. (1999)

Table 2. Spectral Bands for Continuum Slope β

Band	Log λ	λ [Å]
1	3.024 - 3.025	1056.818 - 1059.254
2	3.033 - 3.038	1078.947 - 1091.440
3	3.042 - 3.044	1102.539 - 1106.624
4	3.047 - 3.048	1114.295 - 1116.863
5	3.059 - 3.066	1145.513 - 1164.126

Table 3. Physical Parameters of Young Stellar Populations obtained from FUV Spectral Synthesis

Galaxy	Age [Myr]	α	Z_{code}	β_{obs}^a	$E(B-V)_i$	$\text{Log}(M_*)^b$ [M_\odot]	$F(1150)^c$ [$\times 10^{-14}$]
IRAS 08339+6517	7.0±0.3	2.35	Z_\odot	3±2	0.30±0.15	10±2	7.9±0.8
IRAS 19245+4140	5.0±1.0	2.35 ^d	0.4 Z_\odot	-4±1	0.1±0.1	6 ⁺² ₋₀	6±2
IZw 18	>7	2.20 ^e	<0.2 Z_\odot	-2.1±0.9	0.0±0.1	6 ⁺¹ ₋₀	2±1
M 83	3.5±0.5	2.35 ^c	2 Z_\odot	-1.0±0.7	0.08±0.08	6.2±0.8	60±6
Mrk 054	10±1	2.35 ^c	Z_\odot	-1±2	0.1±0.1	8 ⁺² ₋₀	0.5±0.3 ^f
Mrk 153	6.5±1.0	2.35 ^c	0.2 Z_\odot	-2.8±0.5	0.07±0.05	7.2±0.6	4.2±0.4
NGC 1140	5.0±1.0	2.80	Z_\odot	-1.1±0.5	0.08±0.08	7.5±0.8	14±1
NGC 1667	4.0±1.0	2.35 ^c	2 Z_\odot	-0.9±0.9	0.08±0.08	<7±1	1.0±0.5
NGC 1672	3.5±1.0	2.35 ^c	2 Z_\odot	0±1	0.15±0.10	<7±1	4.3±0.4
NGC 1705	>7.5	2.35 ^c	0.4 Z_\odot	-3.2±0.2	0.01±0.01	6.3 ^{+0.2} _{-0.0}	40±4
NGC 3310	18±2	2.35	2 Z_\odot	0.3±0.3	0.05±0.05	8.1±0.5	40±6
NGC 3504	2.5 ⁺¹ ₋₀	2.35 ^c	2 Z_\odot	1.1±0.4	0.30±0.05	8.8±0.5	4.9±0.5
NGC 3690	6.5±0.5	2.35	Z_\odot	-0.3±0.4	0.15±0.05	8.5±0.5	7.0±0.7
NGC 3991	4.0±0.5	2.80	Z_\odot	1.1±0.9	0.3±0.1	10±1	14±1
NGC 4194	5.5±0.5	2.35 ^c	Z_\odot	3±1	0.4±0.1	10±1	1.6±0.2
NGC 4214	5.5±1.0	2.35 ^c	0.4 Z_\odot	-0.4±0.3	0.13±0.03	6.3±0.3	35±9
NGC 4449-Nuc	10±1	3.30	Z_\odot	-2.7±0.2	0.01±0.01	6.2±0.1	22±2
NGC 4449-H II	5.0±0.5	3.30	Z_\odot	-2.8±0.2	0.01±0.01	6.2±0.1	40±6
NGC 5194	3.5±1.0	2.35 ^c	2 Z_\odot	1±1	0.25±0.15	7±1	5±3
NGC 5253	5.5±1.0	2.35 ^c	0.4 Z_\odot	-1.6±0.5	0.05±0.05	5.4±0.5	11±2
NGC 7496	2.5±0.5	2.35 ^c	2 Z_\odot	-1.8±0.5	0.03±0.02	<5.7±0.2	2.5±0.3
NGC 7673	6.5±0.5	2.35	Z_\odot	-0.9±0.7	0.07±0.07	7±1	7.3±0.7
NGC 7714	4.5±0.3	2.35 ^c	Z_\odot	-0.9±0.5	0.1±0.1	8±1	8.5±0.9
Tol 0440-381	5.0±1.0	2.35 ^c	Z_\odot	0±2	0.20±0.15	9±2	2.0±0.2 ^e

^a FUV Continuum slope measured after correction for Galactic extinction.

^b **Stellar mass values derived from FUV spectra are strongly dependent on data quality and extinction. See text for details.**

^c Corrected for Galactic extinction only. Flux in $\text{ergs s}^{-1} \text{cm}^{-2} \text{\AA}^{-1}$.

^d Standard IMF slope ($\alpha=2.35$) adopted due to S/N or other. See text for details.

^e IMF slope adopted from Aloisi et al. (1999).

^f Extrapolated value because of the redshift.

Table 4. Predicted Parameters for the Young Stellar Populations based on the FUV

Galaxy	Log[#O]	WR/O	Log[F(H α)] ^a	EW(H α) [Å]	EW(4686) [Å]	Log[F(5500)] ^a
IRAS 08339+6517	0	0	-10 ⁺² ₋₂	22 ⁺¹¹³ ₋₈	0	-11 ⁺² ₋₂
IRAS 19245-4140	4 ⁺² ₋₀	0.07 ^{+0.01} _{-0.07}	-12 ⁺² ₋₀	460 ⁺⁶⁰⁰ ₋₂₈₀	3 ⁺¹⁴ ₋₃	-15 ⁺² ₋₀
IZw 18	0	0	-14 ⁺¹ ₋₀	13 ⁺⁹⁵ ₋₁₀	0	-15 ⁺¹ ₋₀
M 83	3.8±0.8	0.3 ^{+0.3} _{-0.1}	-10.8±0.8	550 ⁺³⁷⁰ ₋₇₀	18 ⁺¹⁵ ₋₆	-13.3±0.8
MRK 054	0	0	-14 ⁺² ₋₀	11 ⁺⁶ ₋₀	0	-15 ⁺² ₋₀
MRK 153	4.6±0.6	0	-12.0±0.6	300 ⁺¹⁰⁰ ₋₀	0	-14.3±0.6
NGC 1140	4.6±0.8	0.1 ^{+0.2} ₋₀	-11.5±0.8	200 ⁺⁴⁰⁰ ₋₀	15 ⁺¹⁴ ₋₉	-13.7±0.8
NGC 1667	<5.0 ^{+0.5} ₋₁	0.6 ⁺² _{-0.4}	-11.9 ^{+0.5} ₋₁	480 ⁺⁴⁴⁰ ₋₀	80 ⁺⁰ ₋₇₀	-14.4 ^{+0.5} ₋₁
NGC 1672	<5±1	0.3 ^{+0.4} _{-0.1}	-11±1	550 ⁺⁷⁰⁰ ₋₇₀	20 ⁺⁶⁰ ₋₁₀	-14±1
NGC 1705	0	0	-13.3 ^{+0.2} ₋₀	5 ⁺¹⁵ ₋₃	0	-13.7 ^{+0.2} ₋₀
NGC 3310	0	0	-13.2±0.5	0.5 ⁺² _{-0.3}	0	-13.1±0.5
NGC 3504	6.5±0.5	0.1 ^{+0.2} _{-0.1}	-9.5±0.5	1250 ⁺⁷⁵⁰ ₋₇₀₀	7 ⁺¹⁰ ₋₇	-12.3±0.5
NGC 3690	5.0±0.5	1 ⁺⁰ ₋₁	-11.1±0.5	140 ⁺¹⁸⁰ ₋₁₂₀	6 ⁺¹ ₋₆	-13.1±0.5
NGC 3991	8±1	0.07 ^{+0.08} ₋₀	-9±1	500 ⁺³⁰⁰⁰ ₋₀	16 ⁺²⁸ ₋₀	-12±1
NGC 4194	7.0±1	0.3 ^{+0.6} _{-0.2}	-9.0±1	520 ⁺⁰ ₋₂₇₀	11 ⁺⁹ ₋₄	-12±1
NGC 4214	3.9±0.3	0.15 ^{+0.15} _{-0.15}	-10.4±0.3	400 ⁺⁵⁰⁰ ₋₃₀₀	10 ⁺¹⁵ ₋₇	-13.2±0.3
NGC 4449-Nuc	0	0	-13.2 ^{+0.2} ₋₀	11 ⁺⁶ ₋₀	0	-14.0 ^{+0.1} ₋₀
NGC 4449-HII	2.7 ^{+0.2} ₋₀	0.12 ^{+0.18} ₋₀	-11.8 ^{+0.2} ₋₀	247 ⁺⁵⁰⁰ ₋₀	20 ⁺²⁴ ₋₉	-13.9 ^{+0.2} ₋₀
NGC 5194	5±2	0.3 ^{+0.4} _{-0.2}	-10±2	550 ⁺⁷⁰⁰ ₋₇₀	20 ⁺³⁰ ₋₁₀	-13±2
NGC 5253	3.0±0.5	0.15 ^{+0.15} _{-0.15}	-11.5±0.5	400 ⁺⁵⁰⁰ ₋₃₀₀	10 ⁺¹⁵ ₋₇	-14.2±0.5
NGC 7496	<3.1 ^{+0.5} ₋₀	0.10 ^{+0.10} _{-0.08}	-12.6 ^{+0.5} ₋₀	1250 ⁺³⁸⁰ ₋₃₃₀	7±5	-15.5 ^{+0.5} ₋₀
NGC 7673	3 ⁺² ₋₀	1 ⁺⁰ ₋₁	-13 ⁺² ₋₀	140 ⁺¹⁸⁰ ₋₁₂₀	6 ⁺¹ ₋₆	-15 ⁺² ₋₀
NGC 7714	5±1	0.19 ⁺⁰ _{-0.07}	-11±1	748 ⁺⁰ ₋₅₀₀	44 ⁺⁰ ₋₂₈	-14±1
TOL 0440-381	6 ⁺² ₋₁	0.1 ^{+0.8} _{-0.1}	-12 ⁺² ₋₁	250 ⁺⁵⁰⁰ ₋₀	20 ⁺²⁴ ₋₁₃	-14 ⁺² ₋₁

^a Fluxes in ergs s⁻¹ cm⁻² Å⁻¹.

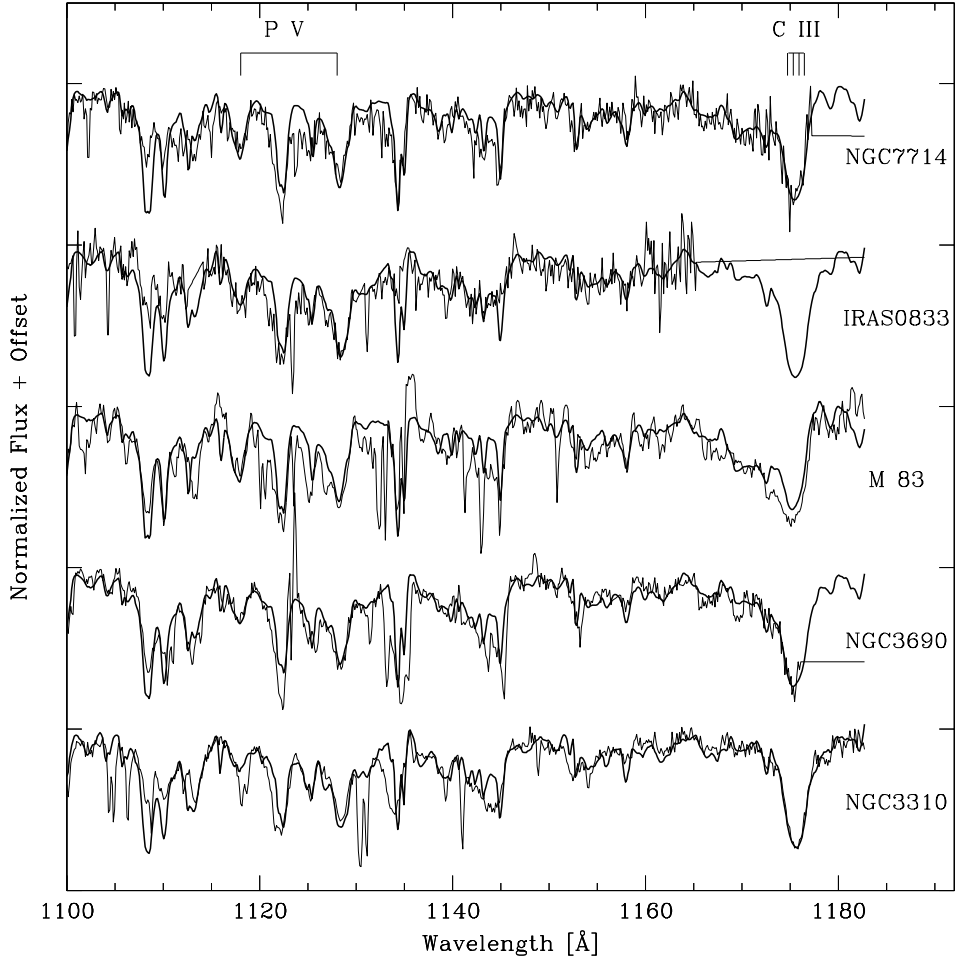


Figure 1. FUSE spectra of well-known starburst galaxies. Thin lines represent the FUSE spectra and thick lines are the best `LavalSB` synthetic spectra obtained for an instantaneous bursts with a standard IMF (i.e. $\alpha = 2.35$ and stars from 1 to $100 M_{\odot}$). From top to bottom: NGC 7714 superimposed on a model having 4.5 Myr and Z_{\odot} ; IRAS 08339+6517 and a model at 7.0 Myr and Z_{\odot} ; M 83 and a model at 3.5 Myr and $2 Z_{\odot}$; NGC 3690 and a model at 6.5 Myr and Z_{\odot} ; and NGC 3310 superimposed on the best-fitting model having 18 Myr at $2 Z_{\odot}$ and $\alpha(\text{IMF})=2.35$.

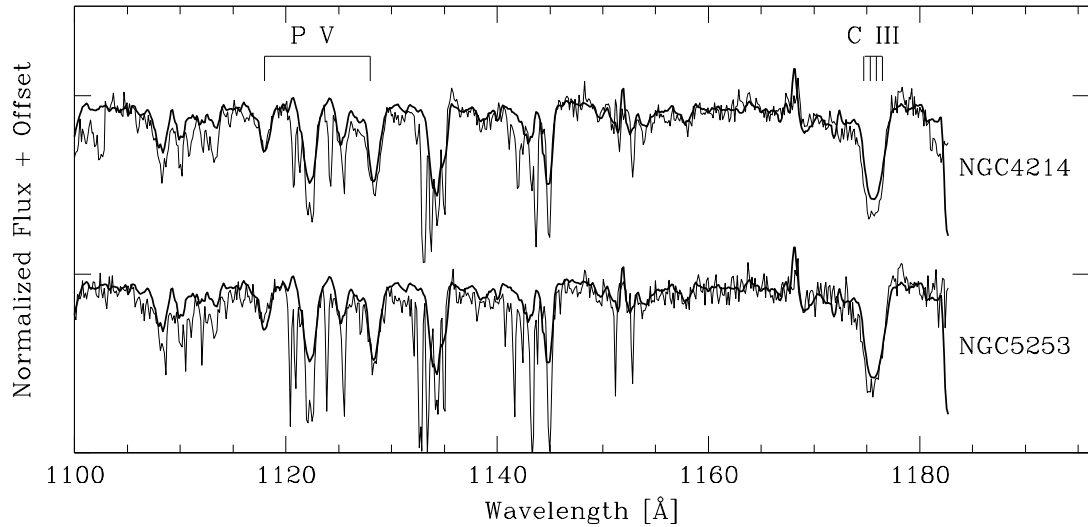


Figure 2. FUSE spectra of NGC 4214 and NGC 5253. Thin lines represent the FUSE spectra and thick lines are *LavalSB* synthetic spectra obtained for a single instantaneous burst with a standard IMF (i.e. $\alpha = 2.35$ and stars from 1 to $100 M_{\odot}$). Top: NGC 4214 superimposed on a model having 4.5 Myr and $0.4 Z_{\odot}$. Bottom: NGC 5253 superimposed on a model having 4.5 Myr and $0.4 Z_{\odot}$.

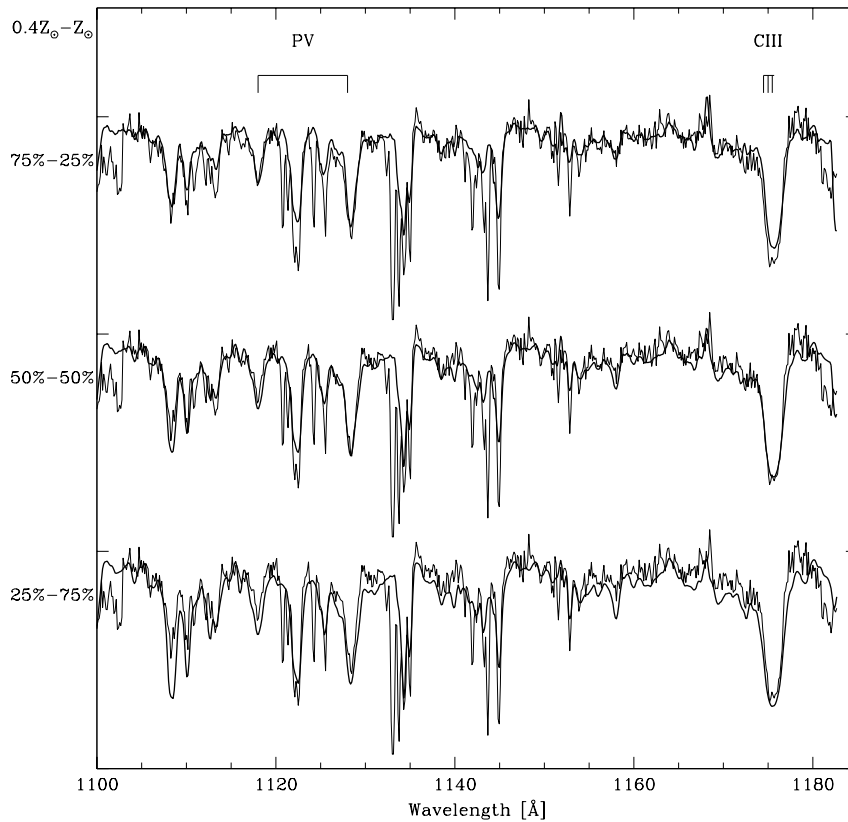


Figure 3. FUSE spectrum of NGC 4214 superimposed on two burst models combining $0.4 Z_{\odot}$ and Z_{\odot} metallicities. Both synthetic populations have 5.5 Myr and a standard IMF. Flux proportions for each combination are indicated on the left, in percents. Thick line: result of combinations. Thin line: NGC 4214 spectrum.

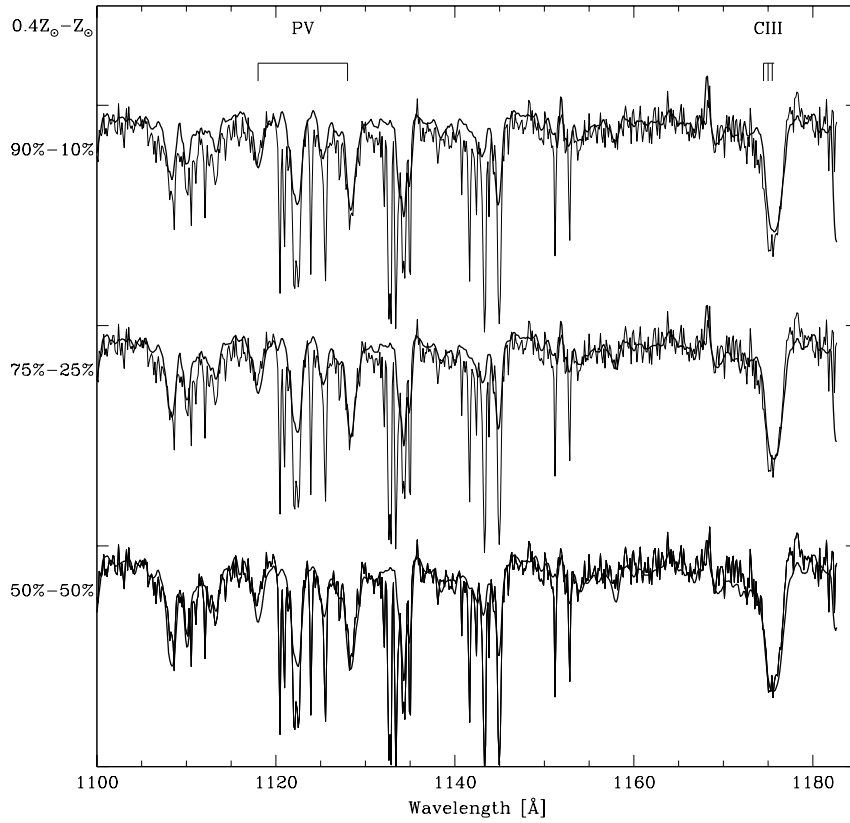


Figure 4. FUSE spectrum of NGC 5253 superimposed on two burst models combining $0.4Z_{\odot}$ and Z_{\odot} metallicities. Both synthetic populations have 5.5 Myr and a standard IMF. See Figure 3 for legend.

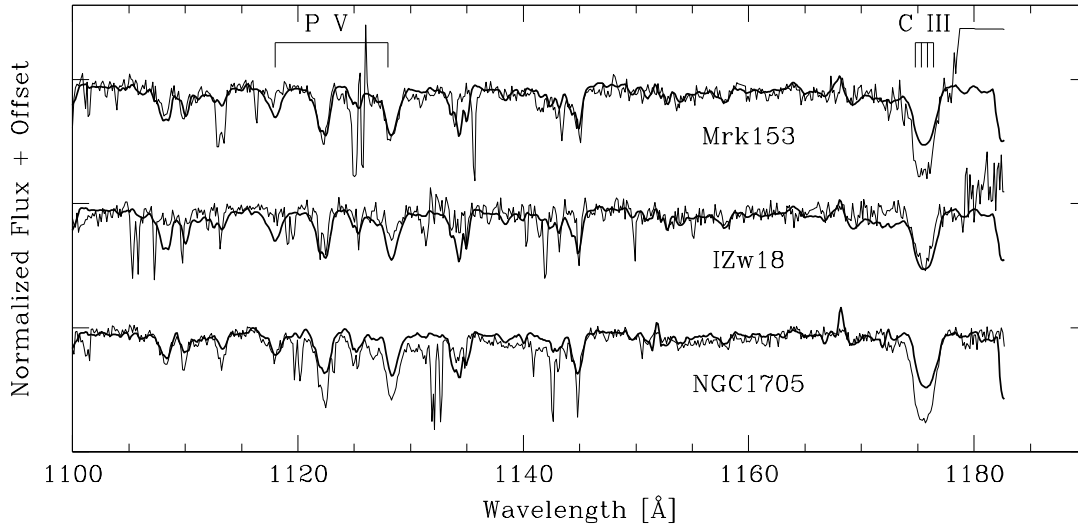


Figure 5. FUSE spectra of starbursts with low metallicity. From top to bottom: Mrk153 superimposed on a model having 6.5 Myr and $0.2Z_{\odot}$; NGC 1705 superimposed on a model having 7.0 Myr at $0.4Z_{\odot}$ and $\alpha(\text{IMF})=2.35$; IZw 18 superimposed on a model having 7.0 Myr at $0.2Z_{\odot}$ and $\alpha(\text{IMF})=2.2$. Thin lines: FUSE spectra; thick lines: LavalSB synthetic spectra of instantaneous bursts.

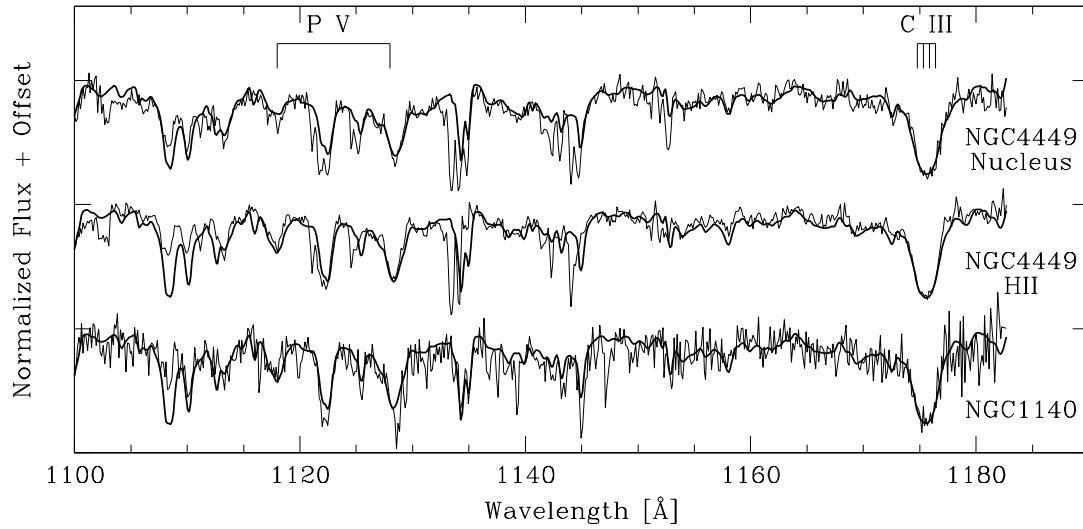


Figure 6. FUSE spectra of starbursts with steep IMF. From top to bottom: Nucleus of NGC 4449 superimposed on the best-fitting model having 10.0 Myr at Z_{\odot} and $\alpha(\text{IMF})=3.3$; H II region of NGC 4449 superimposed on the best-fitting model having 5.0 Myr at Z_{\odot} and $\alpha(\text{IMF})=3.3$; NGC 1140 superimposed on the best-fitting model having 5.0 Myr at Z_{\odot} and $\alpha(\text{IMF})=2.8$. Thin lines: FUSE spectra; thick lines: LavalSB synthetic spectra of instantaneous bursts.

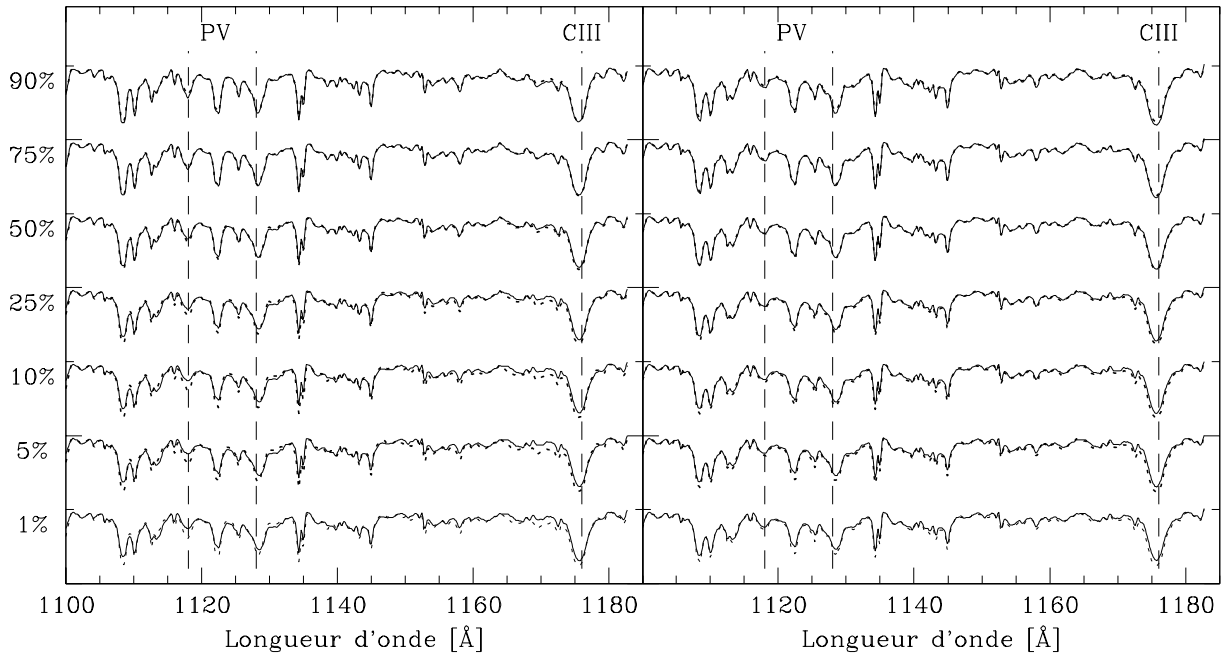


Figure 7. Dilution of a 5.0 Myr burst (left panel) and of a 10.0 Myr burst (right panel) with a 20 Myr burst. Solid line: combination of two single population models of 5.0 and 20 Myr with both standard IMF. The FUV flux proportion of the youngest population is indicated on the left. Dotted line: single synthetic population of 5.0 and 10.0 Myr having $\alpha(\text{IMF})=3.3$.

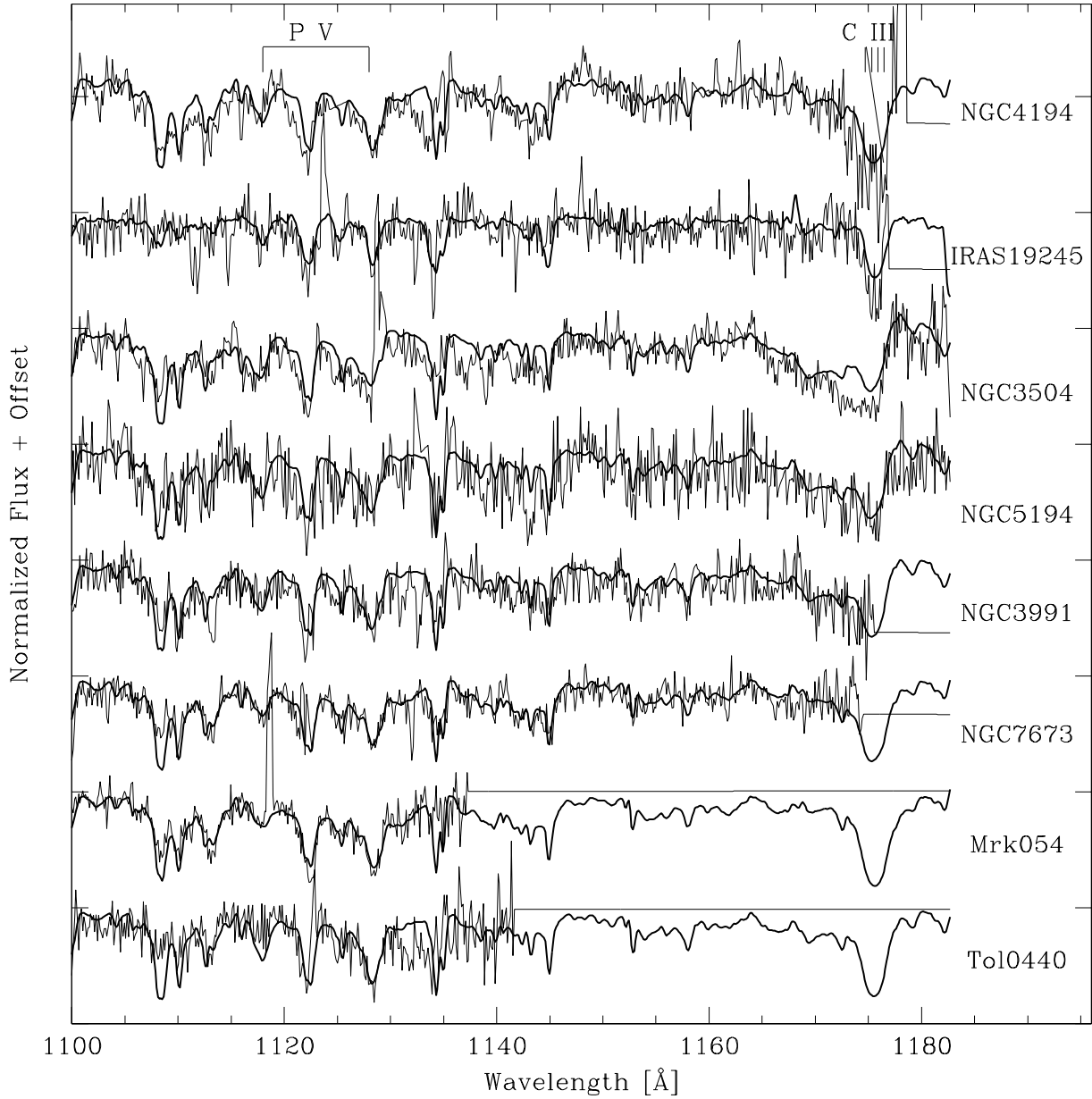


Figure 8. FUSE spectra of starbursts with lower signal-to-noise ratios. From top to bottom: NGC 4194 superimposed on the best-fitting model having 5.5 Myr at Z_{\odot} and $\alpha(\text{IMF})=2.35$; IRAS 19245-4140 superimposed on the best-fitting model having 5.0 Myr at $0.4 Z_{\odot}$ and $\alpha(\text{IMF})=2.35$; NGC 3504 superimposed on the best-fitting model having 2.5 Myr at $2 Z_{\odot}$ and $\alpha(\text{IMF})=2.35$; NGC 5194 (nucleus+H II region) superimposed on the best-fitting model having 3.5 Myr at $2 Z_{\odot}$ and $\alpha(\text{IMF})=2.35$; NGC 3991 superimposed on the best-fitting model having 4.0 Myr at Z_{\odot} and $\alpha(\text{IMF})=2.8$; NGC 7673 superimposed on the best-fitting model having 6.5 Myr at Z_{\odot} and $\alpha(\text{IMF})=2.35$; Mrk 054 superimposed on the best-fitting model having 10.0 Myr at Z_{\odot} and $\alpha(\text{IMF})=2.35$; and Tol 0440-381 superimposed on the best-fitting model having 5.0 Myr at Z_{\odot} and $\alpha(\text{IMF})=2.35$. Thin line: FUSE spectra; thick line: LavalSB synthetic spectra of instantaneous bursts.

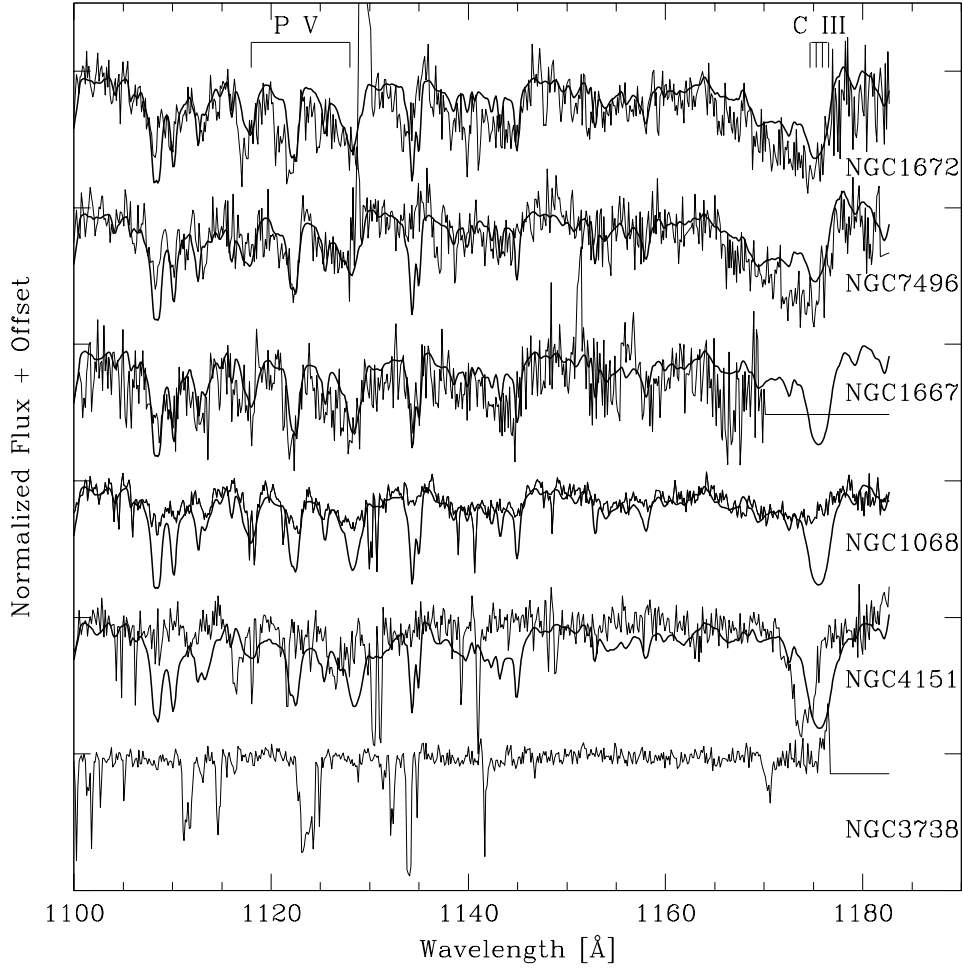


Figure 9. FUSE spectra of Seyfert galaxies. From top to bottom: NGC 1672 superimposed on the best-fitting model having 3.5 Myr at $2Z_{\odot}$ and $\alpha(\text{IMF})=2.35$; NGC 7496 superimposed on the best-fitting model having 2.5 Myr at $2Z_{\odot}$ and $\alpha(\text{IMF})=2.35$; NGC 1667 superimposed on the best-fitting model having 4.0 Myr at $2Z_{\odot}$ and $\alpha(\text{IMF})=2.35$; NGC 1068 superimposed with a Z_{\odot} model for comparison; NGC 4151 in a low-level activity phase with a Z_{\odot} model for comparison; NGC 3783 with no stellar line. In NGC 4151, the massive stellar content (if any) is diluted by the non-thermal radiation (see text). Thin line: FUSE spectra; thick line `Lava1SB` synthetic spectra of instantaneous bursts.